sustainability

MDPI

Article

Impact of ENVI-met-Based Road Greening Design on Thermal Comfort and $PM_{2.5}$ Concentration in Hot–Humid Areas

Meng Du, Yang Zhao *, Jiahao Yang, Wanying Wang, Xinyi Luo, Ziyu Zhong and Bixue Huang

School of Architecture and Urban Planning, Guangzhou University, 230 Guangzhou Higher Education Mega Center West Outer Ring Road, Panyu District, Guangzhou 510006, China
* Correspondence: zhaoyang@gzhu.edu.cn

Abstract: Road greening markedly impacts road thermal comfort and air quality. However, previous studies have primarily focused on thermal comfort or $PM_{2.5}$ individually, with relatively few addressing both aspects comprehensively, particularly in humid regions. This study combined field measurements and simulations. It employed physiological equivalent temperature (PET) and quantified the horizontal distribution of particulate matter 2.5 ($PM_{2.5}$). The research examines the effects of planting spacing, tree species, and tree–shrub combinations on pedestrian walkways in humid climates during both summer and winter. Using measured tree data and road $PM_{2.5}$, a plant model was established and pollution emission parameters were set to validate the effectiveness of the ENVI-met through fitting simulations under various scenarios. The results indicated that (1) plant spacing for trees influenced both the road thermal environment and $PM_{2.5}$ levels. Smaller spacing improved thermal conditions but increased $PM_{2.5}$. (2) trees with large canopies and high leaf area indices (LAIs) notably enhanced thermal comfort, while those with smaller canopies and dense understories facilitated $PM_{2.5}$ dispersion. The 3 m spacing resulted in a maximum absolute $PM_{2.5}$ concentration difference (C) of 5.05 $\mu g/m^3$ in summer and a maximum mean absolute $PM_{2.5}$ concentration difference (M) in the downwind region of 2.13 $\mu g/m^3$ in winter. (3) Combining trees with shrubs moderately improved pedestrian thermal comfort. However, taller shrubs elevated $PM_{2.5}$ concentrations on walkways; heights ranging from 1.5 m to 2 m in summer showed higher C values of 5.38 $\mu g/m^3$ and 5.37 $\mu g/m^3$. This study provides references and new perspectives for the optimization of roadway greening design in humid areas in China.

Keywords: outdoor thermal comfort; road greening; sidewalk trees; ENVI-met; $PM_{2.5}$

Citation: Du, M.; Zhao, Y.; Yang, J.; Wang, W.; Luo, X.; Zhong, Z.; Huang, B. Impact of ENVI-met-Based Road Greening Design on Thermal Comfort and $PM_{2.5}$ Concentration in Hot–Humid Areas. *Sustainability* **2024**, *16*, 8475. https://doi.org/10.3390/su16198475

Academic Editor: Steve Kardinal Jusuf

Received: 12 August 2024
Revised: 20 September 2024
Accepted: 27 September 2024
Published: 29 September 2024

1. Introduction

With the acceleration of urbanization, urban environments continuously deteriorate, exacerbating the urban heat island effect and air pollution [1,2], which threaten urban residents' physical and mental health [3,4]. Particulate matter 2.5 ($PM_{2.5}$), a significant contributor to air pollution [5], primarily originates from vehicle exhaust emissions on urban roads [6] and can cause respiratory and cardiovascular diseases [7].

Vegetation is crucial in mitigating the urban heat island effect and enhancing thermal comfort [8]. Optimizing urban green spaces is an effective way of alleviating the heat island effect and improving thermal comfort. In addition, trees can remove atmospheric pollutants by adsorbing particulate matter through their rough-textured leaves [9]. However, trees can also affect airflow and pollutant dispersion [10,11]. Therefore, an inappropriate road greening design may adversely impact air quality. When designing road greening, comprehensive consideration of the multifaceted effects on thermal comfort and air quality is necessary.

Increasing tree density can provide more shading and enhance the shading effect [12], thereby creating a more comfortable walking environment and increasing pedestrian walking frequency [13]. As tree spacing decreases, mean radiant temperature (T_{mrt}) decreases

exponentially, improving thermal comfort [14]. However, a higher tree density results in poor ventilation, limiting the pollutants' dispersion [15]. $PM_{2.5}$ concentration increases with vegetation density, especially at low wind speeds and when the wind direction is perpendicular to the road [16]. Additionally, different tree species with various physical characteristics affect thermal comfort and $PM_{2.5}$ concentrations differently. Trees with larger canopies are more effective at reducing temperatures and improving thermal comfort [17]. However, they can impede air circulation, leading to the accumulation of $PM_{2.5}$ in street canyons [18]. Trees enhance thermal comfort more effectively than shrubs and grasses, with trees improving physiological equivalent temperature (PET) by approximately 2.4 folds that of ground cover plants and 1.5 folds that of shrubs [19]. However, shrubs increase PET and decrease outdoor thermal comfort at pedestrian height [20]. Regarding $PM_{2.5}$, shrubs are more conducive to pollutant dispersion in street canyons and are the most effective at removing $PM_{2.5}$ at breathing height [21]. Moreover, combining trees with hedges was found to be more effective in reducing road particulate matter [22]. Therefore, in road greening design, planting methods are crucial and require consideration of tree spacing, tree species, and combinations of trees and shrubs.

The ability of trees to improve the outdoor thermal environment is region-specific [23,24] and heavily influenced by local climatic conditions [23]. Guangzhou has a distinct hot and humid climate with rapid urbanization and high population density [25], leading to increasingly prominent air quality issues [26]. Urban residents are vulnerable to extreme heat and $PM_{2.5}$ pollution. Current research mostly focuses on either thermal comfort or $PM_{2.5}$, with relatively few studies examining the combined impact of both.

Using four roads in Guangzhou University Town, we aimed to explore the effects of road greening on outdoor thermal comfort and $PM_{2.5}$ under typical summer and winter climatic conditions in China's hot and humid regions. Finding a roadway greening design strategy that balances thermal comfort and $PM_{2.5}$ concentration through a comprehensive analysis of planting spacing, tree species, and tree–irrigation combinations. Our findings provide scientific and reasonable recommendations for road greening design in hot and humid areas of China for improved urban environment and pedestrian experience.

2. Materials and Methods

2.1. Climate Conditions and Study Areas

Guangzhou (23°08′ N, 113°19′ E) is a typical city in the hot and humid regions of China. It experiences hot and humid summers and warm winters, with an annual average temperature of 22.2 °C and humidity of 77.5% in 2023 [27]. The hottest period is from June to September, with average temperatures ranging from 28.2 to 29.2 °C. January is the coldest month, with an average temperature of 14.3 °C [28]. In summer, Guangzhou is influenced by subtropical high and low pressures in the South China Sea, resulting in prevailing southeasterly winds. In winter, the city experiences prevailing north winds owing to cold high-pressure systems, with higher average wind speeds in winter and lower speeds in summer (Data obtained on 18 September 2024, from https://www.weather-atlas.com/zh/china/guangzhou-climate).

Guangzhou University Town is located on Xiaoguwei Island in the Panyu District, Guangzhou, Guangdong Province. The roads were categorized into four types based on their structure and greenbelt configurations [29]: one roadbed and two belts (R12), two roadways and three belts (R23), three roadways and four belts (R34), and four roadways and five belts (R45), as shown in Figure 1. There were no industrial pollution sources within or near the university town, and vehicular emissions were the primary source of $PM_{2.5}$.

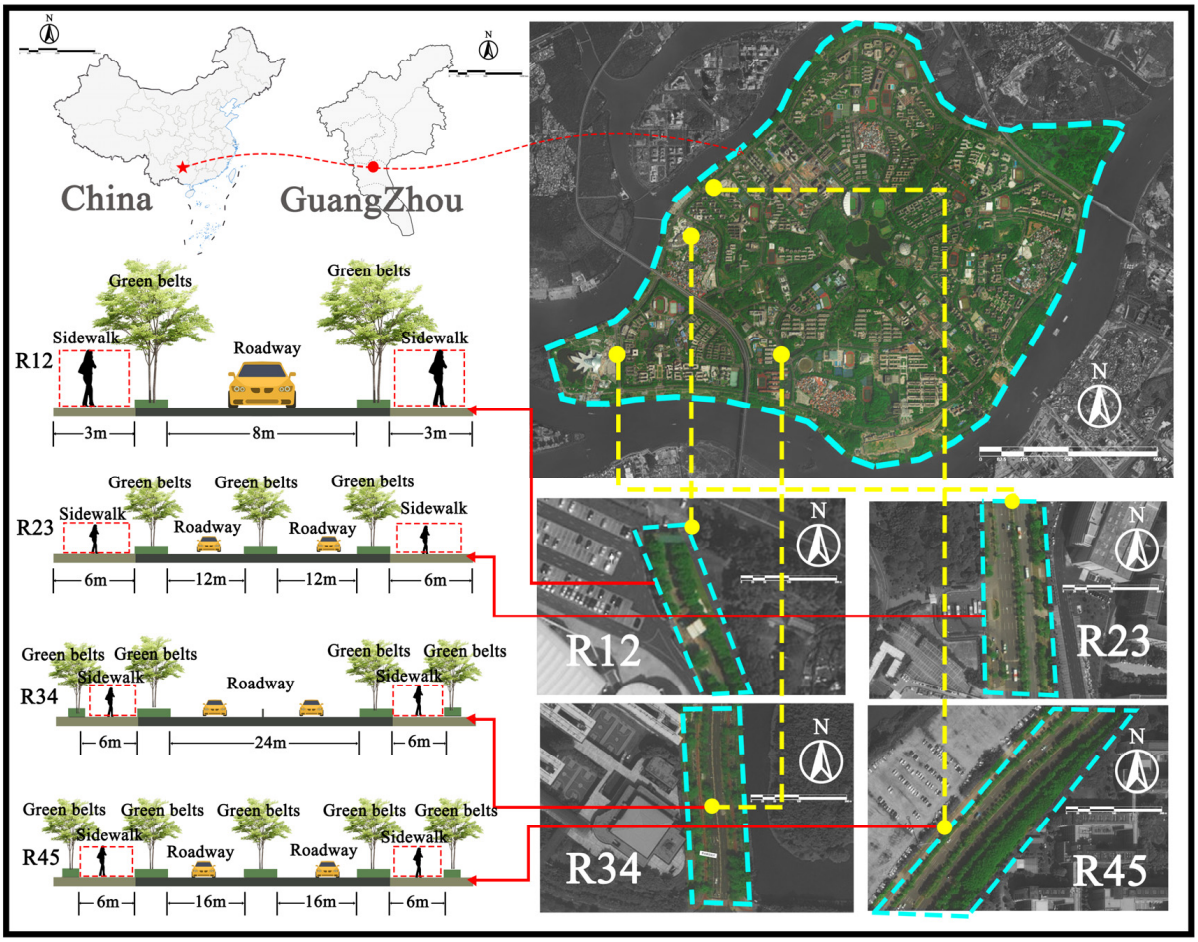

Figure 1. Study area and road types.

2.2. Field Measurements and Model Validation

This study focused on four different types of roads in Guangzhou University. First, traffic flow data were collected using high-definition cameras to capture traffic volumes and corresponding vehicle types on the four roads. Second, on-site measurements were conducted from 8:00 to 17:00 on 20,21,24 and 25 September 2023, and 21, 22, 24, and 25 January 2024. The greenbelt planting configurations along the four roads can be categorized into tree–shrub combinations, tree-only planting, and areas without trees or shrubs. Accordingly, three measurement points were established along each route, located in the tree–shrub combination area, the tree-only area, and the area without trees or shrubs, respectively. The measurement height for all points was set at 1.5 m, as shown in Figure 2. Thermal environment parameters and $PM_{2.5}$ concentrations were collected using a thermal comfort meter and an all-in-one gas detector. $PM_{2.5}$ data were collected hourly from each measurement point, with monitoring lasting > 5 min [30]. The hourly background atmospheric data for the same day were obtained from the Guangzhou Municipal Environmental Protection Bureau. The measurement instruments and their parameters are listed in Table 1. Background meteorological data during the experimental period, including air temperature (T_a), relative humidity (RH), and wind speed (Ws), were collected using a thermal comfort meter set up in an open area 100 m away. Additionally, road width, green belt width, greening configuration, and planting spacing in the study area were measured.

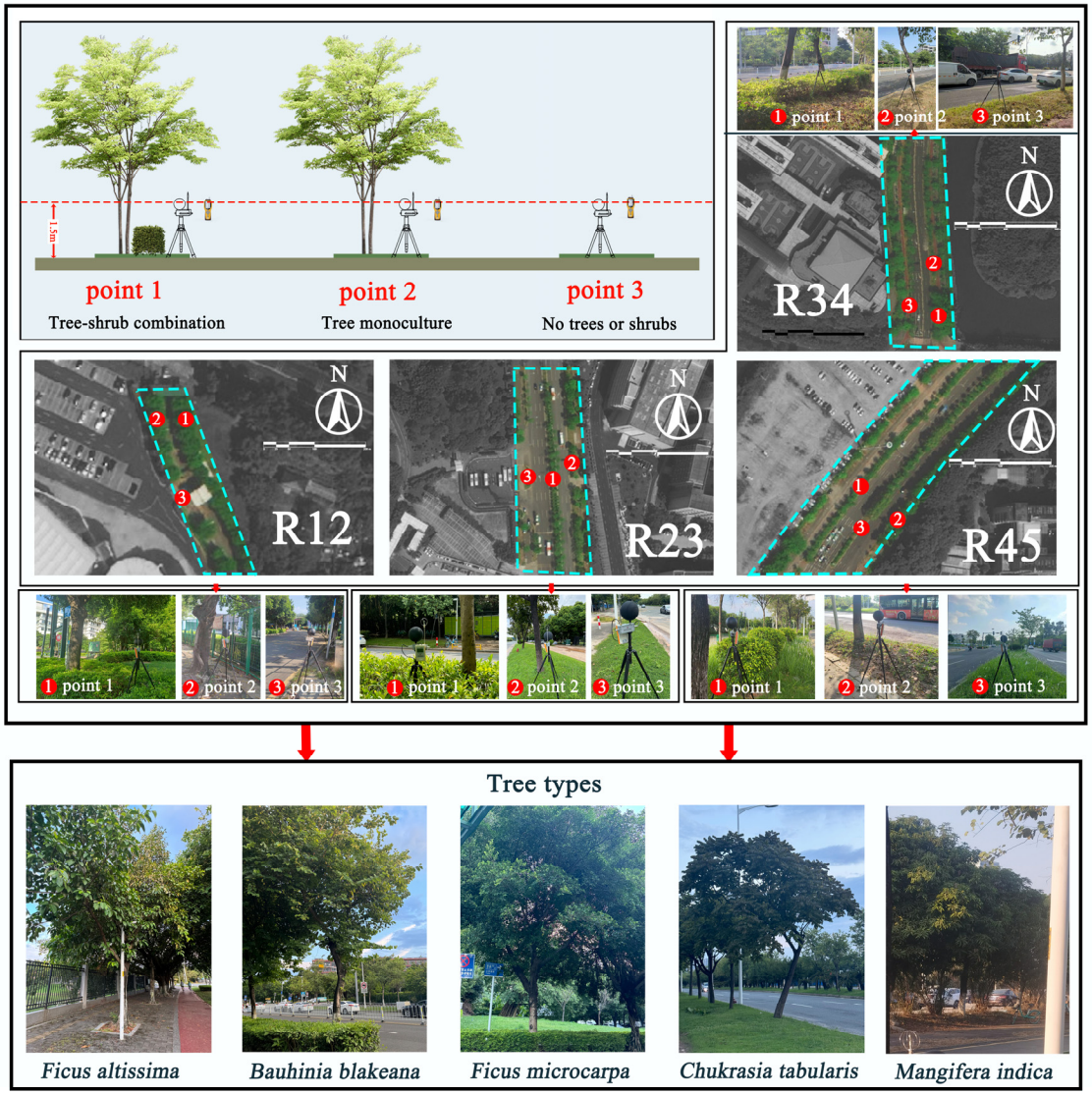

Figure 2. Measurement points and road environments.

Table 1. Information on experimental equipment.

Equipment	Manufacturer	Country of Origin	Model	Parameter	Measuring Range	Accuracy	Sampling Rate
Thermal comfort instrument	Beijing Tianjian Huayi Science and Technology Development Co., Ltd. (Beijing, China)	China	SSDZY-1	Ta (°C)	−20.0–80.0 °C	±0.3 °C	1 min
				RH (%)	0.01–99.9% RH	±2%	1 min
				GlobeTemperature (°C)	−20.0–80.0 °C	±0.3 °C	1 min
				Ws (m/s)	0.05–5.00 m/s	5% ± 0.05 m/s	1 min
All-in-one gas detector	Shenzhen Keruino Electronics Technology Co., Ltd. (Shenzhen, China)	China	GT-1000-B3	$PM_{2.5}$ (μg/m^3)	0–9999 μg/m^3	±3% μg/m^3	10 s

The reliability of the ENVI-met model was validated by comparing the temperature, humidity, and $PM_{2.5}$ concentration values obtained from on-site measurements with the model's output values. The accuracy of the model was evaluated using the correlation coefficient (R^2), root mean square error (RMSE), and mean absolute error (MAE). The calculation formulas (1) are as follows:

$$RMSE = \sqrt{\frac{\sum_{i=1}^{n} \left(X_{obs,i} - X_{model,i}\right)^2}{n}} \quad (1)$$

$$MAE = \frac{\sum_{i=1}^{n} \left|X_{obs,i} - X_{model,i}\right|}{n} \quad (2)$$

where X_{obs} represents the observed values, X_{model} represents the values simulated by the software, and n represents the number of data points.

2.3. Modeling and Parameter Setting

Based on the satellite images and on-site measurement data of the case area, physical three-dimensional models of each road were constructed using the ENVI-met space module. Each road was set to a length of 300 m, with a grid resolution of 3 m × 3 m ×3 m. Three-dimensional vegetation models were established according to the actual conditions of the model. The building surface materials were set to concrete, and the road materials were set according to the actual conditions (Table A1).

Additionally, the model used the measured wind direction and speed. The pollutant source settings in the ENVI-met were configured using the hourly traffic volume for each road. The hourly pollution source emission rate was estimated using equation (3) [31]:

$$Q = C \cdot E \quad (3)$$

where Q ($\mu g/m^3$) represents the pollutant emission rate; C (veh/h) denotes the hourly traffic flow, which were 390 veh/h, 243 veh/h, 220 veh/h, and 207 veh/h for the R12, R23, R34, and R45 roads, respectively; and E stands for the $PM_{2.5}$ emission factor, mg/(km·veh). The average emission factor for Guangzhou is 57.8 mg/(km·veh) [32]. Based on Formula (4), the average emission rates per hour are 3.32 $\mu g/m^3$, 3.53 $\mu g/m^3$, 3.90 $\mu g/m^3$, and 6.30 $\mu g/m^3$ for the R12, R23, R34, and R45 roads, respectively. Pollutants are emitted across the entire width of the road at a height of 0.3 m (the height of vehicle exhaust pipes).

Because of the effective simulation capability of ENVI-met for $PM_{2.5}$ concentrations over a short period of time [33], simulations were conducted in three stages (8:00–10:00, 11:00–14:00, and 15:00–17:00) after preheating, totaling 8 measurement days.

2.4. Case Studies

2.4.1. Establishment of Arbor Database

To accurately predict the impact of roadside greening on outdoor thermal comfort and $PM_{2.5}$ concentration in humid subtropical regions, this study selected nine common tree species in Guangzhou: *Michelia alba* (Ma), *Ficus altissima* (Fa), *Bauhinia blakeana* (Bb), *Mangifera indica* (Mi), *Alstonia scholaris* (As), *Chukrasia tabularis* (Ct), *Dracontomelon duperreanum* (Dd), *Ficus concinna* (Fc), *Cinnamomum camphora* (Cc). The ENVI-met Albero model contains nine parameters: leaf area density, tree height, under-canopy height, leaf reflectance, crown width, root area density, root depth, root morphology, and root width. Previous studies have indicated that area density, width, root depth, and morphology have insignificant effects on the simulation of outdoor thermal environments [34]; thus, default values were used in model construction. Tree height, under-canopy height, and crown width were measured using a rangefinder, while leaf shortwave reflectance was measured using a spectrophotometer (Lambda950). The leaf area index (LAI) was determined using

TOP-1300, while the leaf area density (LAD) values at different heights within the tree canopy were calculated using the following formula (4) [35]:

$$LAD = \int_0^x L_m \left(\frac{h - Z_m}{h - Z}\right)^n exp\left[n\left(\frac{h - Z_m}{h - Z}\right)\right] dZ \quad (4)$$

where $0 \leq Z \leq Z_m$ with $n = 6$ with $Z_m \leq Z \leq h$ with $n = 0.5$

The tree model and parameters are illustrated in Figure 3.

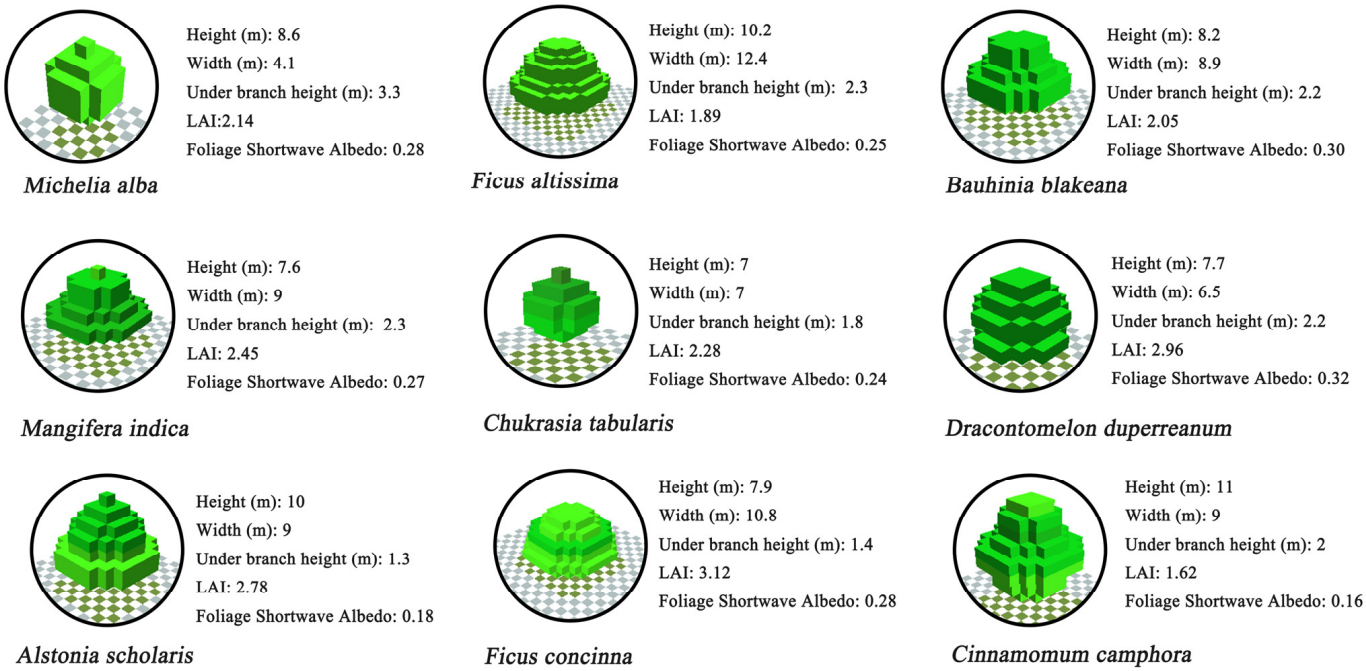

Figure 3. Joe model and parameters.

2.4.2. Case Studies

As shown in Figure 4, the study was divided into three phases: determining the optimal planting spacing, selecting the best tree species, and combining trees with shrubs. First, 3 m, 6 m, and 9 m planting spacing were arranged as As on the four roads. The reference group consisted of roads with no lane trees. The models used were R12-As-3, R12-As-6, R12-As- 9, R23-As-3, R23-As-6, R23-As-9, R34-As-3, R34-As-6, R34-As-9, R45-As-3, R45-As-6, and R45-As-9. Second, nine types of lane tree species commonly found in Guangzhou were arranged on the green belts of the four roads. The reference group consisted of a road model without trees. Third, after comparing the tree species, two were selected and combined with or without shrubs of different heights: 1 m, 1.5 m, and 2 m. The combinations were labeled as Ma-1.5, Ma-2, As-0, As-1, As-1.5, and As-2.

The T_a, T_{mrt}, Ws, and $PM_{2.5}$ concentrations of the pedestrian space of each model were determined. The BIO-met process was used to calculate the PET value for each scenario. The parameters were set to 35 years old, 75 kg weight, and 1.75 m height, and clothing insulation values in summer and winter were 0.5 Clo and 0.9 Clo, respectively. The metabolic rate was 164.7 W. The results were taken as a means of follow-up analysis.

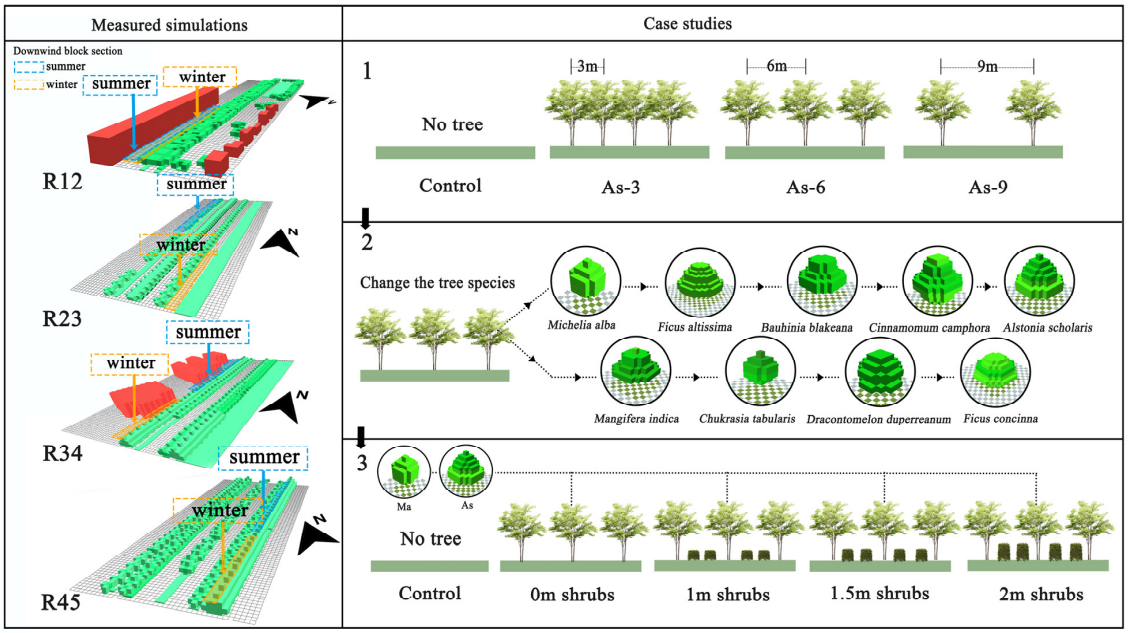

Figure 4. ENVI-met model and the three stages of simulation.

2.5. Thermal Comfort Evaluation Index and Quantitative Analysis of $PM_{2.5}$

2.5.1. PET

Common thermal indices include the Standard Effective Temperature (SET*), Wet Bulb Globe Temperature (WBGT), Predicted Mean Vote (PMV) index, and Physiological Equivalent Temperature (PET) [36]. PET, derived from the human energy balance equation, considers environmental factors such as T_a, RH, Ws, and T_{mrt}, as well as personal factors such as clothing and metabolic rate, to comprehensively assess human thermal comfort [37]. The residents of hot and humid regions exhibit higher adaptability and tolerance to such environments [38]. Therefore, this study used PET to assess the thermal comfort in Guangzhou, as shown in Table 2. The ranges for PET assessment in Guangzhou were obtained from [39].

Table 2. The ranges for PET assessment in Guangzhou.

PET Value	Thermal Sensation	Grade of Physiological Stress
-	Very cold	Extreme cold stress
-	Cold	Strong cold stress
Below 11.3 °C	Cool	Moderate cold stress
11.3–19.2 °C	Slightly cool	Slight cold stress
19.2–24.6 °C	Comfortable	No thermal stress
24.6–29.1 °C	Slightly warm	Slight heat stress
29.1–36.3 °C	Warm	Moderate heat stress
36.3–53.6 °C	Hot	Strong heat stress
Above 53.6 °C	Very hot	Extreme heat stress

2.5.2. Quantification of $PM_{2.5}$ Distribution

When people walk in pedestrian areas, particularly downwind zones, they are more likely to be exposed to roadway pollution [40]. Therefore, the distribution of $PM_{2.5}$ at the heights of people in the downwind areas of roads should be considered. By comparing the control and reference groups in downwind zones, the absolute $PM_{2.5}$ concentration differences for each model and the mean absolute $PM_{2.5}$ concentration difference in downwind areas were calculated using Formulas (5) and (6) as follows:

$$C = a_{xy} - b_{xy} \quad (5)$$

$$M = \frac{\sum_{x=1,x=1}^{x=m,y=n} C}{x \times y} \quad (6)$$

Herein, C (μg/m^3) represents the absolute difference in (x, y) concentration between the control and reference groups at grid coordinates (x, y); a_{xy} denotes the $PM_{2.5}$ in the control group at grid coordinates (x, y) and b_{xy} denotes the $PM_{2.5}$ concentration in the reference group at grid coordinates (x, y); M (μg/m^3) is the mean absolute $PM_{2.5}$ concentration difference in downwind areas, where x and y represent the number of grids, with equal grid counts per road in summer and winter: 50 grids for R12 and 100 grids for R23, R34, and R45.

3. Results

3.1. Testing Results

As shown in Figure 5, during the measurement period, summer T_a ranged from 28.7 °C to 39.5 °C, with an average of 35.3 °C. RH ranged from 47.6% to 77.6%, averaging 61.7%. T_a ranged from 4.4 °C to 26.1 °C, with an average of 12.4 °C in winter. Relative humidity ranged from 32.3% to 78.0%, averaging 55.9% across the four roads, showing noticeable differences. R45 exhibited higher T_a than the other three roads (approximately 11.5 °C higher on average), while R12, R23, and R34 were similar. The RH was higher in R45 and R34 than in R12 and R23. Point 3 (without trees) consistently exhibited a significantly higher T_a than Points 2 and 1 across all four roads in both summer and winter. The RH at Point 1 was generally higher than at Points 2 and 3, with Point 3 exhibiting a comparatively lower RH. The standard deviation, variance, and coefficient of variation are shown in Tables A2 and A3. These results aligned with the typical summer and winter climatic characteristics of Guangzhou.

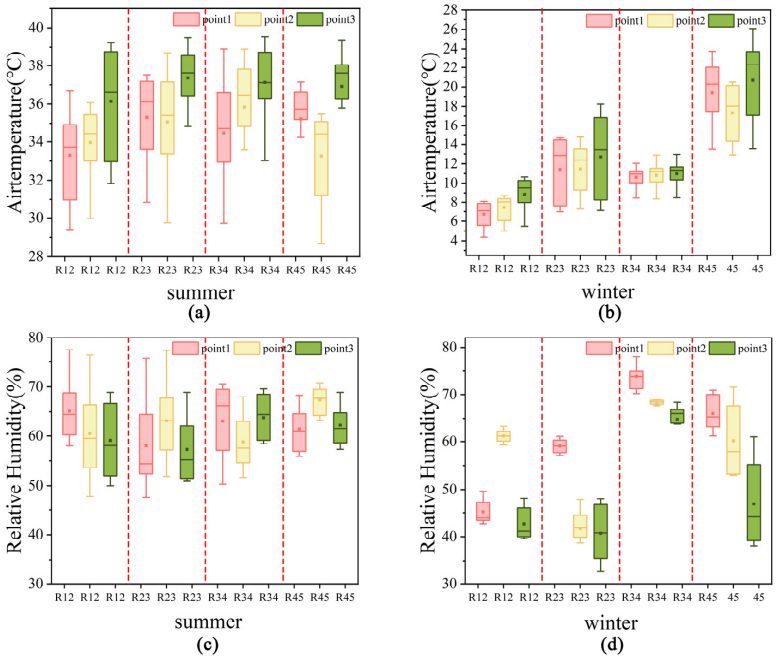

Figure 5. Measured summer air temperature (**a**), winter air temperature (**b**), summer relative humidity (**c**), and winter relative humidity (**d**).

As shown in Figure 6, during the measurement period, the variation in the $PM_{2.5}$ concentration was more pronounced in summer, with each road experiencing different traffic volumes and environmental conditions, resulting in varying $PM_{2.5}$ in the range of 11.97 μg/m^3–44.60 μg/m^3, with a mean value of 25.17 μg/m^3. In winter, the trend in $PM_{2.5}$ concentration was more stable, with overall similar ranges of 1.30 μg/m^3–41.40 μg/m^{33} with a mean value of 28.95 μg/m^3. The $PM_{2.5}$ concentrations on road R34 were more

variable and lower in the afternoon compared to the other three roads. The difference in $PM_{2.5}$ concentrations among the three measurement points is insignificant, with Point 3 being slightly higher than Points 1 and 2. The fluctuations in the data may reflect the effect of the cold weather on the measurement day, which resulted in a significantly more significant variance and coefficient of variation in this data set. The standard deviation, variance, and coefficient of variation are shown in Tables A2 and A3.

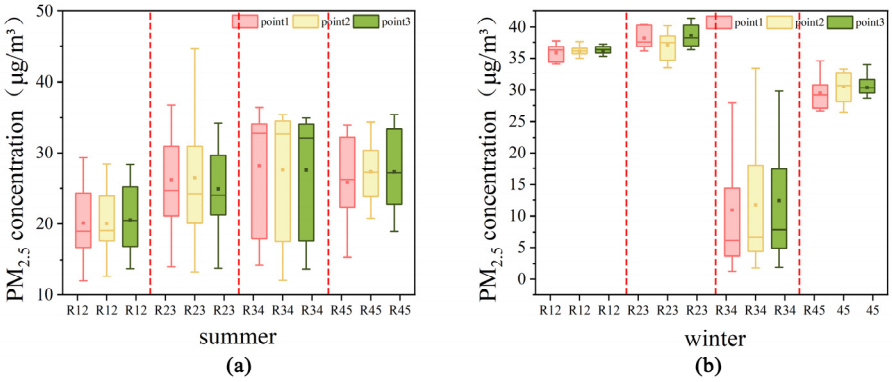

Figure 6. Measured summer $PM_{2.5}$ concentrations (**a**) and winter $PM_{2.5}$ concentrations (**b**).

3.2. Model Accuracy Assessment

Figures 7 and 8 depict the fitting of simulated and measured values of T_a, RH, and $PM_{2.5}$ concentration at each measurement point. In summer, the coefficients of correlation (R^2) for T_a, RH, and $PM_{2.5}$ concentration were 0.73–0.90, 0.71–0.94, and 0.75–0.93, respectively. In winter, the R^2 values for T_a, RH, and $PM_{2.5}$ concentration were 0.72–0.92, 0.7–0.93, and 0.65–0.9, respectively. These results indicate that the established ENVI-met models are reliable and suitable for simulating the distribution of thermal environment and $PM_{2.5}$ concentration in humid climates. Although a small portion of the data had large variance and coefficient of variation due to weather changes, the results of the model accuracy validation based on these raw data showed that the overall prediction accuracy of the model met the requirements. Therefore, these data were still retained to ensure data integrity and reliability.

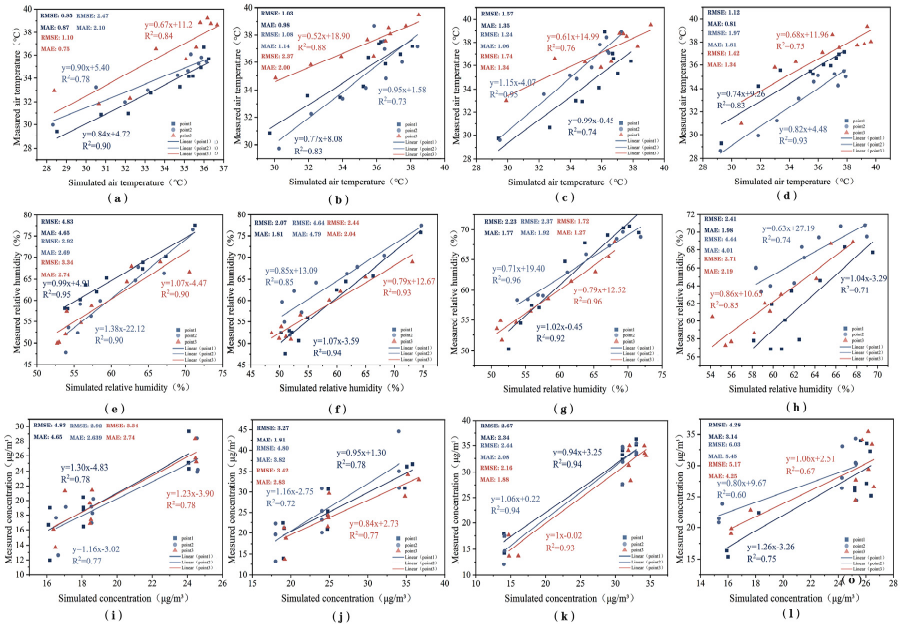

Figure 7. Relationship between simulated air temperature (**a**–**d**), relative humidity (**e**–**h**), $PM_{2.5}$ concentration (**i**–**l**), and the measured value during the summer.

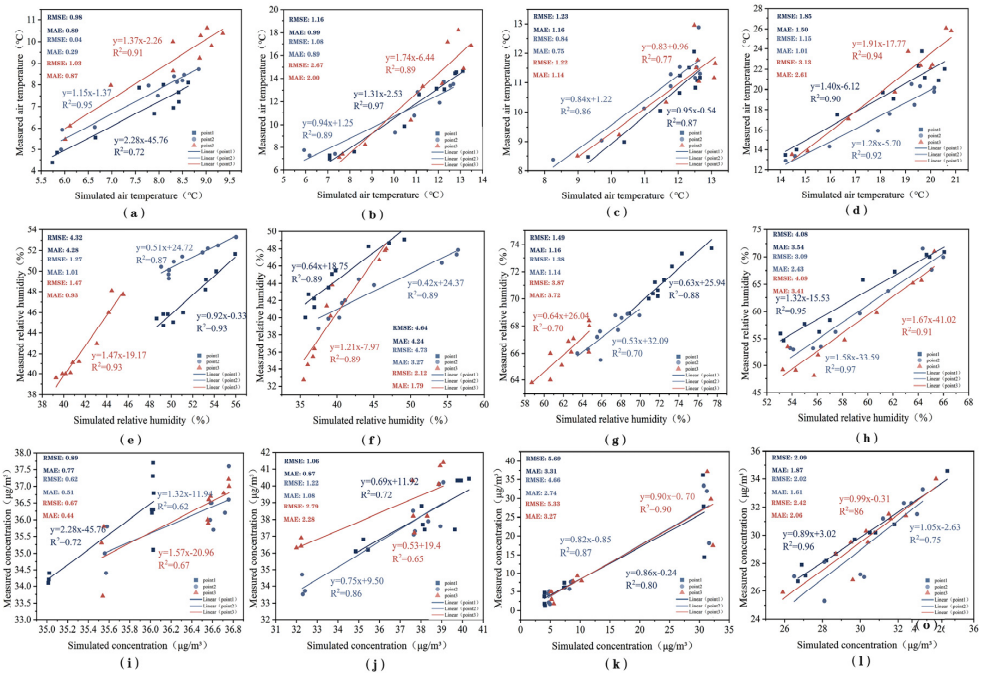

Figure 8. Relationship between simulated air temperature (**a**−**d**), relative humidity (**e**−**h**), $PM_{2.5}$ concentration (**i**−**l**), and measured values during summer.

3.3. Influence of Tree Spacing

3.3.1. Impact of Tree Spacing on the Thermal Environment Parameters

In the simulated scenarios using As (9 m canopy width), the hourly outputs of T_a, T_{mrt}, and Ws were collected and compared across different planting distances. Given that 14:00 represents the peak temperature, the analysis focused on the changes in the thermal environment during this period.

As shown in Figures 9 and 10, three different planting distances on the four roads consistently reduced T_a (T_{mrt}) on pedestrian walkways compared with the control group. The cooling effect was most pronounced with the 3 m planting distance, resulting in summer reductions of 0.2 °C (5.4 °C), 0.5 °C (3.8 °C), 1.0 °C (21.7 °C), and 0.7 °C (17.8 °C) across the four roads, and winter reductions of 0.4 °C (1.5 °C), 0.2 °C (15.0 °C), 0.6 °C (10.9 °C), and 0.7 °C (13.5 °C). The cooling effect diminished gradually at 6 m and 9 m planting distances. Different planting distances significantly influenced the T_{mrt} for R45. Notably, in winter, the 6 m and 9 m planting distances increased T_{mrt} at 14:00 for R12, with the highest increase observed at 6 m (1.8 °C). This could be attributed to the orientation of R12 (north–south–east–west), where winter north winds prevail, and the street trees cannot shade the 2 PM winter sun and reduce wind speeds, increasing T_{mrt}. The 6 m spacing, on the other hand, reduces the wind speed more compared to 9 m and increases T_{mrt} more.

As shown in Figure 11, compared with the control, planting trees at various distances somewhat reduced wind speeds at pedestrian heights, with the effect decreasing in the order 3 m > 6 m > 9 m. The 3 m planting distance reduced Ws in summer by 0.02 m/s (R12), 0.05 m/s (R23), 0.14 m/s (R34), and 0.12 m/s (R45), and in winter by 0.24 m/s (R12), 0.07 m/s (R23), 0.14 m/s (R34), and 0.21 m/s (R45). Dense planting at 3 m caused the most significant decrease in wind speed. Notably, owing to the different prevailing wind directions in summer and winter, R45 experienced the greatest reduction in Ws during summer owing to the planting distance, while R45 and R12 showed more significant reductions in winter.

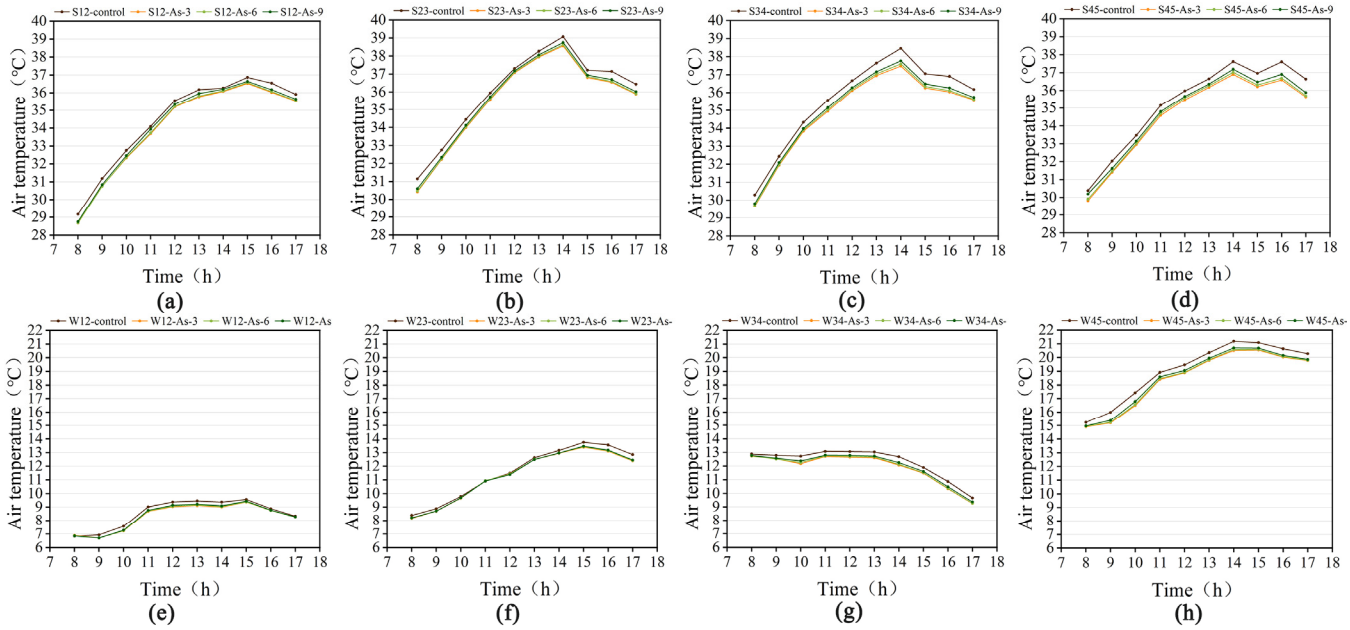

Figure 9. Effects of different planting distances of R12, R23, R34, and R45 on air temperature (T_a) during summer (**a**–**d**) and winter (**e**–**h**).

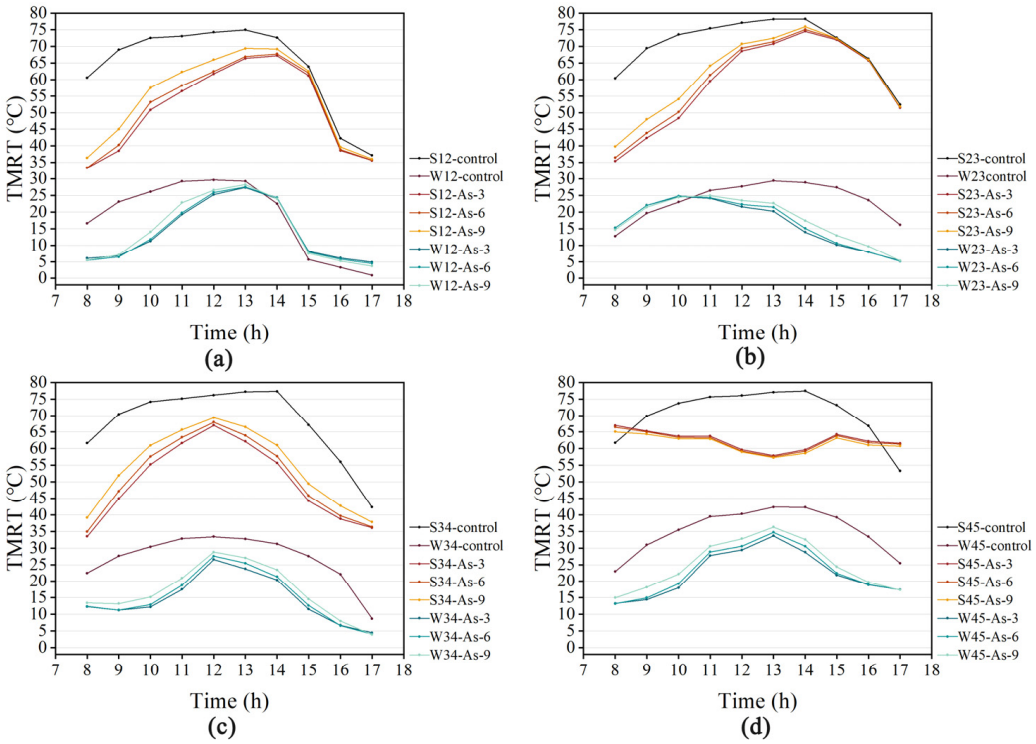

Figure 10. Effects of different planting distances on mean radiant temperature (T_{mrt}) on R12 (**a**), R23 (**b**), R34 (**c**), and R45 (**d**).

3.3.2. Impact of Tree Spacing on PET

Figure 12 summarizes the PET values at different planting distances from 8:00 to 17:00. Planting trees at various distances significantly reduced PET values, with the greatest reduction observed at 3 m spacing, followed by 6 m and 9 m. Compared with the control, during summer, planting As at different distances reduced PET values by up to 20.3 °C (R12-3), 20.2 °C (R12-6), 18.1 °C (R12-9), 17.2 °C (R23-3), 16.6 °C (R23-6), 14.5 °C (R23-9), 17.8 °C (R34-3), 17.0 °C (R34-6), 14.5 °C (R34-9), 17.0 °C (R45-3), 15.7 °C (R45-6), and 11.7 °C

(R45-9). The PET values for R45 were mostly influenced by the 3 m planting distance, with a maximum difference of 5.3 °C, while the least affected was R12, with a difference of 2.1 °C. This effect could be attributed to the higher number of As at 3 m, compared with R12, providing stronger cooling effects. Therefore, the 3 m planting distance showed more significant reductions in PET values, compared with 9 m, which was particularly effective in enhancing thermal comfort during hot summers. In winter, PET values were reduced by up to 3.3 °C (R12-3), 3.2 °C (R12-6), 3.1 °C (R12-9), 12.6 °C (R23-3), 12.4 °C (R23-6), 11.6 °C (R23-9), 5.8 °C (R34-3), 5.6 °C (R34-6), 4.9 °C (R34-9), 5.9 °C (R45-3), 5.5 °C (R45-6), and 4.6 °C (R45-9) when planting at various distances. While all distances reduced PET values, R23, R34, and R45 maintained PET values above 11.3 °C during the daytime, while some PET values for R12 were slightly below 11.3 °C (10.5–11.3 °C), potentially causing discomfort due to cold temperatures. Therefore, planting distances should be carefully considered in colder winter weather for their impact on road PET values, as overly dense tree planting can unexpectedly reduce PET values and increase cold sensation. Roads with more green areas or higher tree densities showed significant distance-related effects.

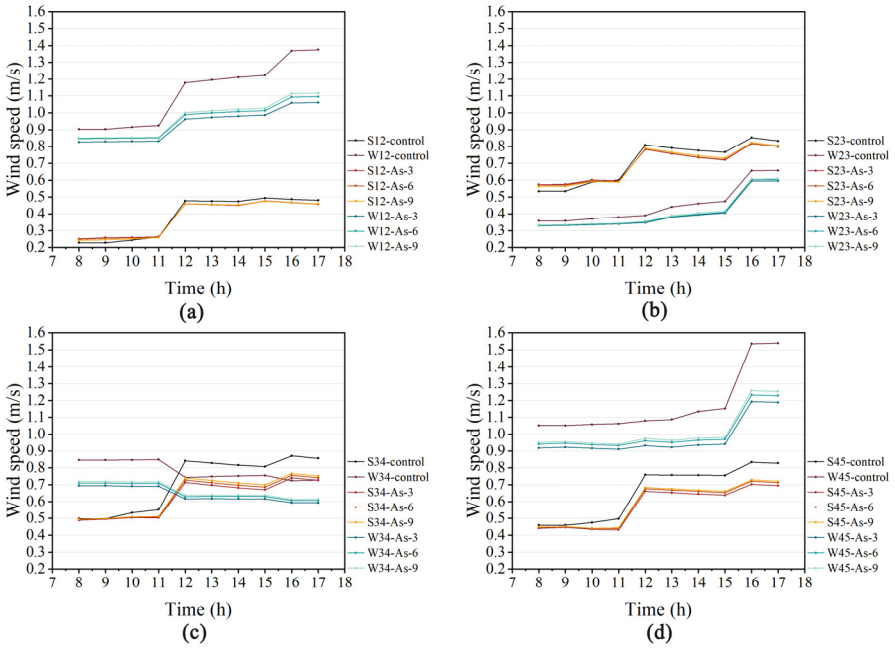

Figure 11. Effects of different spacings on Ws of R12 (**a**), R23 (**b**), R34 (**c**), and R45 (**d**).

At a moderate planting distance of 6 m, Fa and Mi significantly reduced T_a to 1.4 °C (R34 summer) and 1.3 °C (R23 summer); conversely, Ma showed comparatively weaker cooling effects by up to 0.4 °C (R34 summer). The other species exhibited effects between these extremes (Figure A1). Regarding T_{mrt} reduction, Fa and Cc showed the highest cooling effect, reducing T_{mrt} by up to 26.8 °C (R34 summer) and 16.9 °C (R23 winter), whereas Ct and Ma showed the least reduction (Figure A2). Fc significantly impacted wind speeds, reducing them by up to 0.4 m/s (R12 summer), whereas Ma had the smallest impact, reducing wind speeds by up to 0.1 m/s (R12 summer). Other species fell between these extremes in their effects on wind speed (Figure A3).

3.3.3. Effects of Spacing Distance on the Absolute $PM_{2.5}$ Concentration Difference

At 8:00 AM during peak traffic hours, $PM_{2.5}$ concentration changes are particularly significant. Comparing $PM_{2.5}$ variations in different scenarios at this time, as shown in Figure 13, positive values indicate an increase in concentration, whereas negative values indicate the opposite. Regardless of whether it is winter or summer, as the planting spacing increased, $PM_{2.5}$ dispersed from the leeward side to the windward side under the influence of wind, showing a decreasing trend of $PM_{2.5}$ concentration in the order 3 m > 6 m > 9 m.

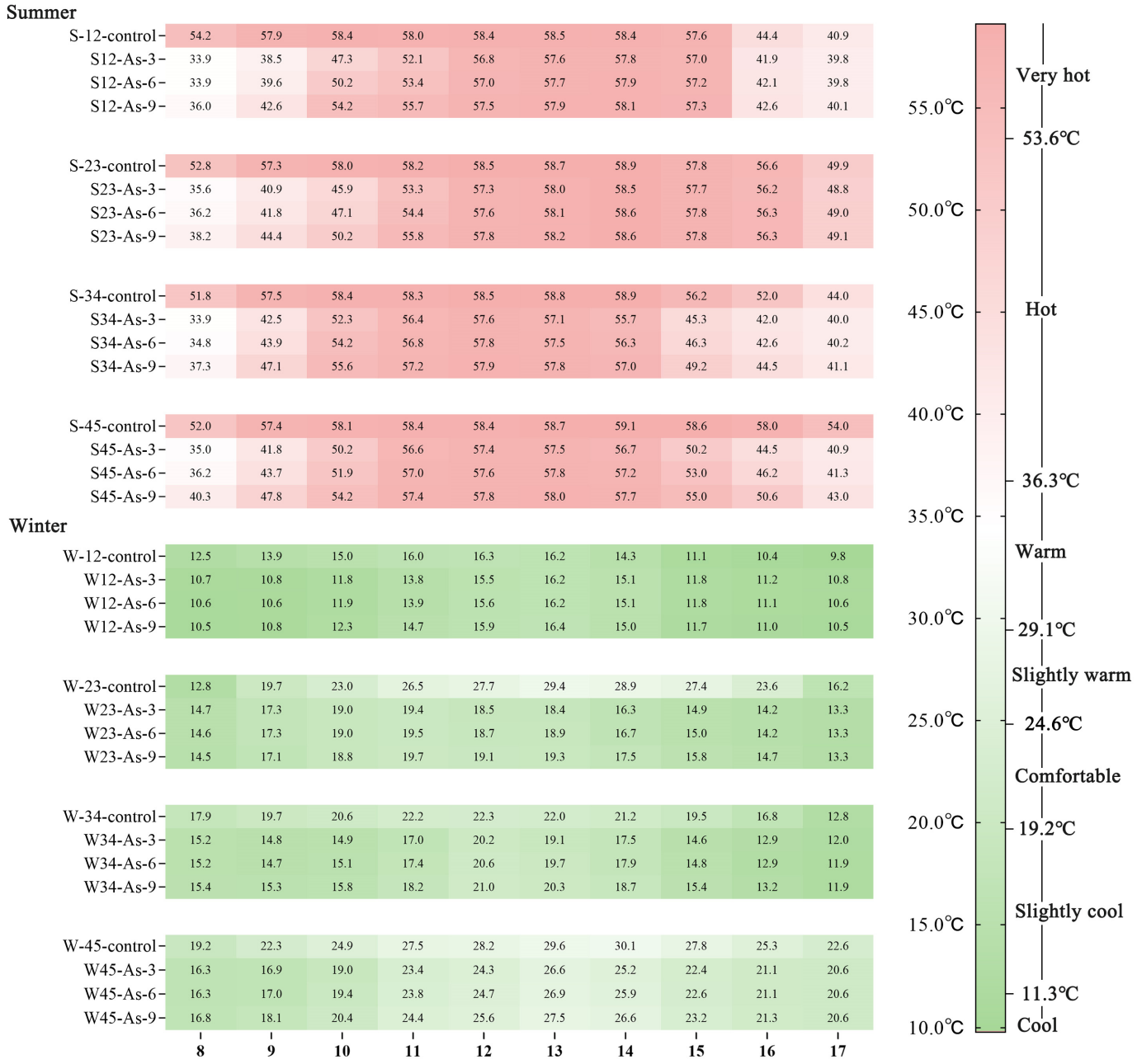

Figure 12. Effect of tree spacing on PET.

In summer, the maximum value for the absolute $PM_{2.5}$ concentration difference (C) reached 5.05 μg/m^3 (R45) when the plant spacing was 3 m. On roads such as R23 and R45, where there are no nearby buildings, natural winds are obstructed by trees, thereby inhibiting $PM_{2.5}$ dispersion. Therefore, smaller plant spacing resulted in higher $PM_{2.5}$. On roads with buildings, such as R12 and R34, both buildings and trees hindered pollutant dispersion, leading to higher $PM_{2.5}$ concentrations in those areas. As a result, smaller planting spacing increases pollution in the pedestrian areas of the roadway, especially on roads with a high number of greenbelts and buildings.

In winter, with a plant spacing of 3 m, the $PM_{2.5}$ concentration significantly increased across the entire neighborhood, especially in areas with lower wind speeds. This effect was exacerbated by both the low wind speeds and the 3 m plant spacing, which hindered $PM_{2.5}$ dispersion. On the R23 road, the C value reached a maximum of 2.13 μg/m^3. Although winter typically has lower overall pollutant concentrations at pedestrian heights

owing to above-average wind speeds compared with summer, different plant spacing still significantly influenced $PM_{2.5}$ pollution from traffic emissions, with smaller spacing exacerbating $PM_{2.5}$ pollution.

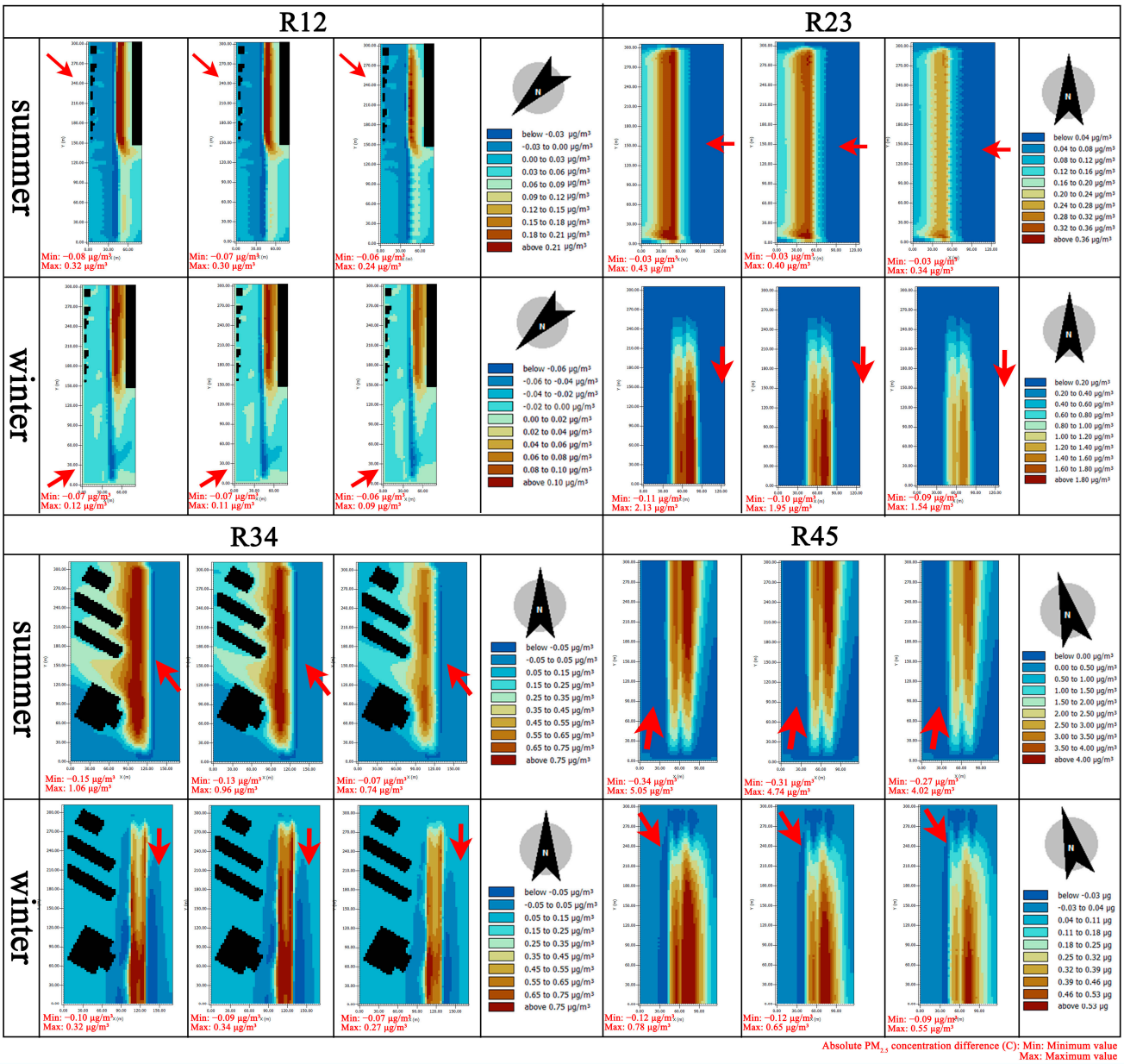

Figure 13. Effect of spacing on the absolute $PM_{2.5}$ concentration difference.

3.3.4. Effect of Tree Spacing on the Mean Absolute $PM_{2.5}$ Concentration Difference in Downwind Areas

As shown in Figure 14, during summer, the mean absolute $PM_{2.5}$ concentration difference(M) for the three spacing intervals on all four roads was greater than 0, indicating an increasing trend in $PM_{2.5}$ concentration downwind. The highest and lowest M values were at 3 m and 9 m spacings, respectively. Among the four roads, R45 exhibited the highest M values: 2.13 $\mu g/m^3$ (3 m), 1.96 $\mu g/m^3$ (6 m), and 1.70 $\mu g/m^3$ (9 m). During winter on R34, all three sets of M values were <0, indicating that tree planting benefits reduction in $PM_{2.5}$ concentration on this road, with 3 m spacing showing slightly better results than 6 m and 9 m spacings. However, the M values for the other three roads remained above 0, with significantly higher M values at 3 m spacing compared with 6 m and 9 m spacings. This

suggests that at 3 m spacing, $PM_{2.5}$ pollution is exacerbated on sidewalks, decreases slightly at 6 m spacing, and disperses more favorably at 9 m spacing. Therefore, when designing roadway landscaping, a larger planting spacing should be selected to minimize pollution due to $PM_{2.5}$ pollution concerns. And in the winter R34 scenario, choosing smaller spacing can instead reduce $PM_{2.5}$ pollution.

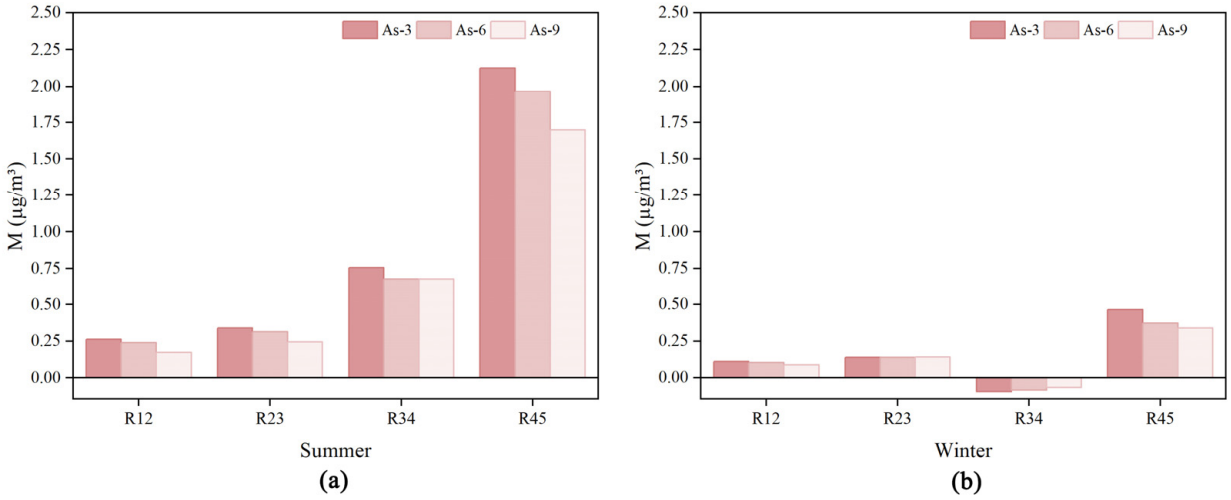

Figure 14. The difference in $PM_{2.5}$ concentration in the lower air area of the sideways and the average value of $PM_{2.5}$ during the summer (**a**) and winter (**b**).

3.4. Impact of Tree Species

Based on the previous section, planting trees with a spacing of 6 m along roadside green belts moderately affected PET and $PM_{2.5}$. This section discusses the influence of different tree species at a 6 m plant spacing on PET and $PM_{2.5}$.

3.4.1. Impact of Tree Species on PET

Figure 15 illustrates the impact of different tree species on PET values along R12, R23, R34, and R45 roads. On R12, compared with the control group, Ma increased PET values by 0.1 °C at 2:00 PM. Other tree species generally decreased PET values, with Fa showing the most significant reduction of up to 1.4 °C. During winter, trees generally increased afternoon PET values by 0.7–1.8 °C, with Mi showing the highest increase, while only Fa decreased PET by 0.9 °C. On R23, during summer, tree species reduced PET values by −0.1–1 °C, with Fa achieving the greatest reduction and Ma causing a slight increase in PET. In winter, various tree species reduced PET by 2.8–6 °C, with Cc achieving the highest reduction and Ct the lowest. For R34 in summer, PET values decreased by 0.4–6.5 °C, and in winter, the decrease ranged from 0.6 °C to 4.3 °C. Fa performed effectively in summer, and Cc was more effective in winter than Ct. In R45, summer PET values decreased by 0.8–3.8 °C, and winter PET values decreased by 1.2–6.6 °C. Fa achieved the most significant reduction, while Ct showed the least reduction.

In conclusion, Fa and Cc effectively reduced the PET values, whereas Ma and Ct showed relatively limited effects. Notably, planting trees on R12 increased the PET values in the area, possibly because of increased T_{mrt} during the afternoon, which is a primary factor influencing thermal comfort [13,41]. Additionally, although tree species markedly reduced PET values during winter, post-planting PET values remained above 11.3 °C throughout most of the day. Therefore, tree species that enhance thermal comfort in the summer should be prioritized.

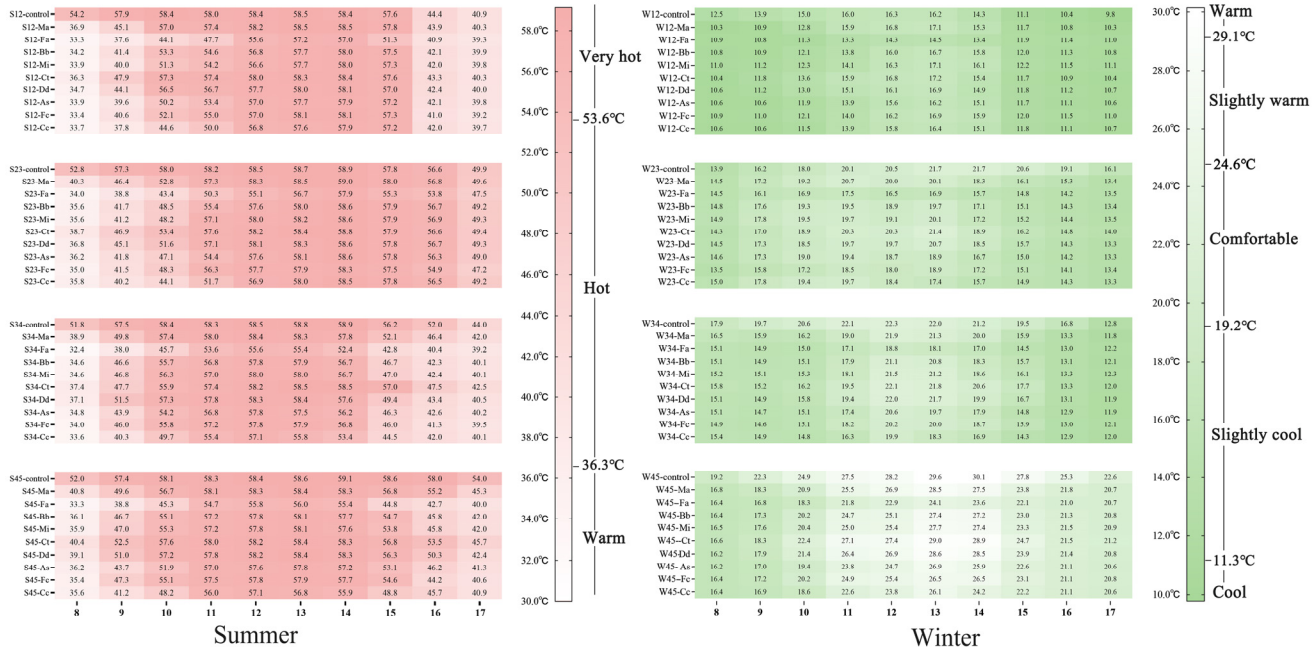

Figure 15. Impact of tree species on the PET value of pedestrian space.

3.4.2. Effects of Tree Species on $PM_{2.5}$ Absolute Concentration Difference

When the planting spacing was 6 m, Figure 16 illustrates the distribution of C values between the different tree species and the control group. Dispersed $PM_{2.5}$ can accumulate in specific areas owing to the obstructive effects of trees and buildings, leading to increased concentrations.

In summer, the maximum C values for $PM_{2.5}$ on the four roads were 0.47 μg/m^3 (Fc), 0.60 μg/m^3 (Fa), 1.54 μg/m^3 (Fa), and 5.99 μg/m^3 (Fa) for R12, R23, R34, and R45 roads, respectively. R12 and R23 roads showed a relatively limited increase in $PM_{2.5}$ concentration, whereas R34 and R45 roads exhibited a significant increase. In winter, the maximum C values for $PM_{2.5}$ on the four roads were 0.31 μg/m^3 (Fc), 3.17 μg/m^3 (Fa), 1.10 μg/m^3 (Fa), and 0.99 μg/m^3 (Fc) for R12, R23, R34, and R45 roads, respectively. The increase in $PM_{2.5}$ concentration was significant on the R23 road and least significant on the R12 road. Across the four roads, $PM_{2.5}$ concentrations notably increased with Fa and Fc, whereas Ma and Ct showed a less significant increase. In summer, the maximum C values were 3.39 μg/m^3 (Ma) and 3.47 μg/m^3 (Ct) on R45, and in winter, they were 1.22 μg/m^3 (Ma) and 1.29 μg/m^3 (Ct) on R23. Bb, Cc, Dd, and As had $PM_{2.5}$ that fell between these two categories of trees.

In addition, to explore the effects of tree morphological indicators on $PM_{2.5}$ concentrations more deeply, the correlations of tree height, crown spread, height under a branch, and LAI with $PM_{2.5}$ concentrations were further analyzed, as shown in Table 3. Calculation of the correlation between morphological indicators of trees and PM2.5 concentrations showed that crown width had the greatest effect on $PM_{2.5}$ concentration, especially in summer, with correlation coefficients of 0.817 ($p < 0.01$) and 0.696 ($p < 0.05$) in the R12 and R34 paths, respectively, showing strong positive correlations. Tree height was also positively correlated with $PM_{2.5}$ concentration in summer, but its effect was slightly weaker than crown height. In winter, the correlation coefficient of tree height in R23 roads reached 0.900 ($p < 0.01$), showing a significant positive correlation. These suggest that increasing tree height and crown spread may increase $PM_{2.5}$ concentrations. Under-branch height had a smaller effect on $PM_{2.5}$ concentrations, while LAI showed a significant negative correlation in winter (R34, −0.800, $p \leq 0.01$), suggesting that larger LAI may contribute to lower $PM_{2.5}$ concentrations. These results suggest substantial differences in the effects of tree morphometric indicators on $PM_{2.5}$ concentrations across seasons and sites, with tree

morphometric indicators having a more significant impact in the summer and a weaker effect in the winter, similar to HE et al. [31].

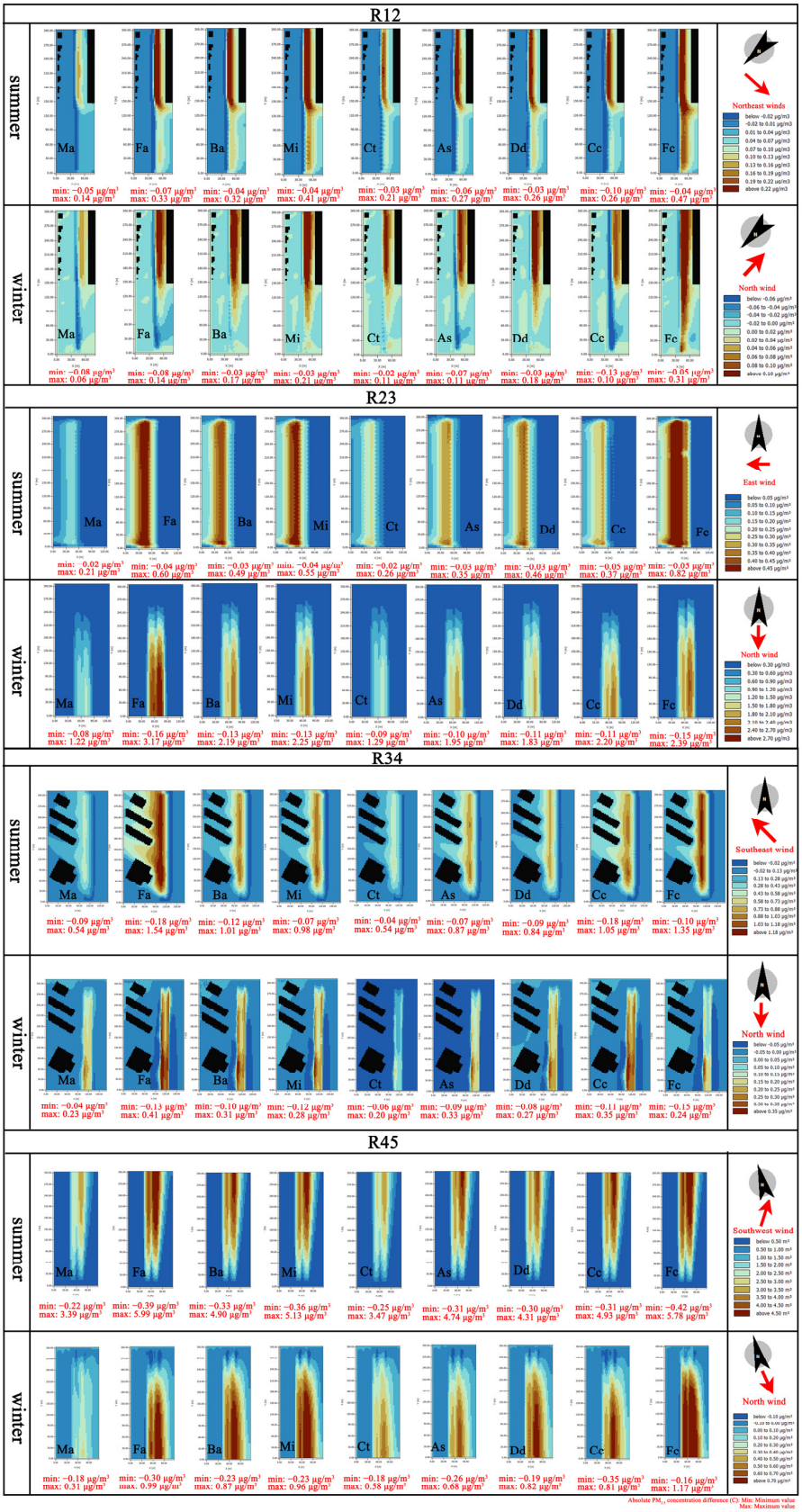

Figure 16. Effects of tree species on $PM_{2.5}$ absolute concentration differences.

Table 3. Calculation of the correlation between morphological indicators of trees and $PM_{2.5}$ concentration. In this table, the symbol '*' indicates $p < 0.05$, and '**' indicates $p < 0.01$.

Summer				Winter			
Tree Morphological Indicators	**Scene**	**Pearson Correlation Coefficient**	***p*-Value**	**Tree Morphological Indicators**	**Scene**	**Pearson Correlation Coefficient**	***p*-Value**
Tree Height	R12	0.703 *	0.035	Tree Height	R12	−0.45	0.224
	R23	0.306	0.424		R23	0.900 **	0.001
	R34	0.721 *	0.028		R34	0.767 *	0.016
	R45	0.772 *	0.015		R45	0.117	0.765
Crown Width	R12	0.817 **	0.007	Crown Width	R12	0.407	0.277
	R23	0.777 *	0.014		R23	0.661	0.053
	R34	0.696 *	0.037		R34	0.017	0.965
	R45	0.669 *	0.049		R45	0.424	0.256
Height Under Branch	R12	0.295	0.44	Height Under Branch	R12	−0.42	0.26
	R23	0.038	0.922		R23	0.311	0.415
	R34	0.335	0.379		R34	0.529	0.143
	R45	0.42	0.26		R45	0.092	0.813
LAI	R12	0.404	0.281	LAI	R12	0.617	0.077
	R23	−0.304	0.426		R23	−0.567	0.112
	R34	−0.558	0.119		R34	−0.8 **	0.01
	R45	−0.534	0.139		R45	−0.053	0.892

Among the simulated tree species, Fa (tree height of 10.2 m, crown spread of 12.4 m) and Fc (crown spread of 10.8) were not conducive to the diffusion of $PM_{2.5}$ due to their physical characteristics (high tree height or large crown spread), which led to an increase in concentration. In contrast, Ma (crown width 5 m), characterized by a narrow canopy, showed the least obstruction of $PM_{2.5}$ dispersion across all four roads. This study indicates that $PM_{2.5}$ concentrations are significantly influenced by tree height and canopy width. Species with large canopy widths are more likely to hinder $PM_{2.5}$ dispersion, thereby increasing $PM_{2.5}$ concentrations on pedestrian pathways.

3.4.3. Effect of Tree Species on the Mean Absolute $PM_{2.5}$ Concentration Difference in the Downwind Area

Figure 17 illustrates the M values of downwind sections. On R12, R23, and R45 roads, both in summer and winter, M values were greater than 0, indicating an increase in $PM_{2.5}$ concentration in pedestrian areas downwind.

As shown in Figure 17a, on the R12 road, the overall $PM_{2.5}$ concentrations slightly increased with M values greater than 0. In summer, the maximum and minimum M values were 0.35 $\mu g/m^3$ (Mi) and 0.12 $\mu g/m^3$ (Ma), respectively, while in winter, the maximum and minimum values were 0.24 $\mu g/m^3$ (Fc) and 0.05 $\mu g/m^3$ (Ma), respectively.

As shown in Figure 17b, during summer on the R23 road, planting Fa (0.47 $\mu g/m^3$), Fc (0.45 $\mu g/m^3$), and Mi (0.43 $\mu g/m^3$) significantly increased $PM_{2.5}$ concentrations on pedestrian paths, with Ma (0.16 $\mu g/m^3$) showing a slight increase. In winter, the overall increases were modest, with Cc contributing relatively more to $PM_{2.5}$ concentrations and Fc (0.10 $\mu g/m^3$) contributing the least.

As shown in Figure 17c, on the R34 road during summer, Fa caused the highest increase in $PM_{2.5}$, with an M value of 1.13 $\mu g/m^3$. Ma induced the smallest increase in $PM_{2.5}$, with an M value of 0.4 $\mu g/m^3$. In winter, street trees generally benefited from the reduction of $PM_{2.5}$ concentration on pedestrian paths, where Fa showed the most significant reduction effect, with an M value of −0.13 $\mu g/m^3$, and Ma exhibited the smallest reduction, with an M value of −0.04 $\mu g/m^3$. The R34 road aligned with the prevailing direction of winter wind from north to south. This facilitated $PM_{2.5}$ dispersion, but street trees mitigated this by restricting $PM_{2.5}$ more to the vehicle lane area, thereby reducing $PM_{2.5}$ concentration on pedestrian paths. Fa, with its broad canopy, showed the most significant obstruction

to $PM_{2.5}$, whereas Ct, owing to its smaller canopy, showed a less pronounced obstruction to $PM_{2.5}$.

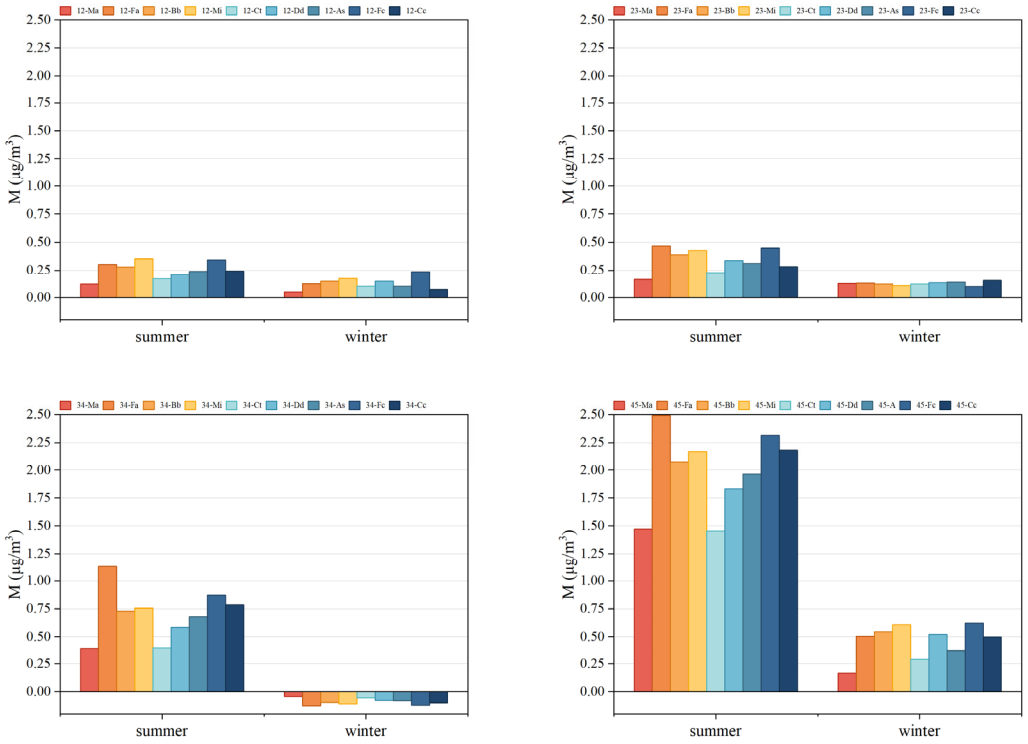

Figure 17. Mean absolute $PM_{2.5}$ concentration difference in the downwind area on R12 (**a**), R23 (**b**), R34 (**c**), and R45 (**d**) roads.

As depicted in Figure 17d, during both summer and winter seasons on the R45 road, M values were greater than 0, leading to an increase in $PM_{2.5}$ concentration on pedestrian paths. Specifically, the M value significantly increased in summer compared with winter, indicating a notable rise in $PM_{2.5}$ concentration on pedestrian paths of R45, exacerbating $PM_{2.5}$ pollution. When Fa was a street tree, M peaked at 2.5 $\mu g/m^3$. Fc, Cc, and Mi showed notably higher M values than other tree species at 2.31 $\mu g/m^3$, 2.18 $\mu g/m^3$, and 2.18 $\mu g/m^3$, respectively, while Ma exhibited the smallest M value at 1.5 $\mu g/m^3$. In winter, Fc, Mi, and Bb exhibited higher M values at 0.62 $\mu g/m^3$, 0.6 $\mu g/m^3$, and 0.54 $\mu g/m^3$, respectively. Because the R45 road does not align parallel to the summer and winter wind directions, $PM_{2.5}$ easily accumulated on vehicle and pedestrian paths owing to obstruction by street trees. Larger and denser canopies of street trees hindered $PM_{2.5}$, thereby exacerbating $PM_{2.5}$ pollution on pedestrian paths.

3.5. Impact of Shrubs on Different Heights

Based on our findings in the previous section, we found that the impact of tree species on heat comfort and the concentration of $PM_{2.5}$ showed opposite trends. Therefore, we selected a tree species (As) that balanced the thermal comfort and $PM_{2.5}$ diffusion and another tree species (Ma) that is less conducive to thermal comfort but facilitates $PM_{2.5}$ diffusion. We then combined these tree species with different types of shrubs for simulation.

3.5.1. Impact of Shrub Height on PET Value

Figure 18 illustrates how the combination of trees and shrubs significantly reduced PET values compared with the control. Specifically, combinations with Ma and various heights of shrubs (0/1/1.5/2 m) resulted in summer PET reductions of approximately 0.84 °C to 0.86 °C and winter reductions of about 2.58 °C to 2.63 °C. Similarly, combinations with As and shrubs at the same heights led to summer PET reductions of 1.93–2.00 °C

and winter reductions of 4.27–4.35 °C. These findings indicate that trees have a greater impact on PET values than shrubs, whereas the height of shrubs has a minimal influence on PET values.

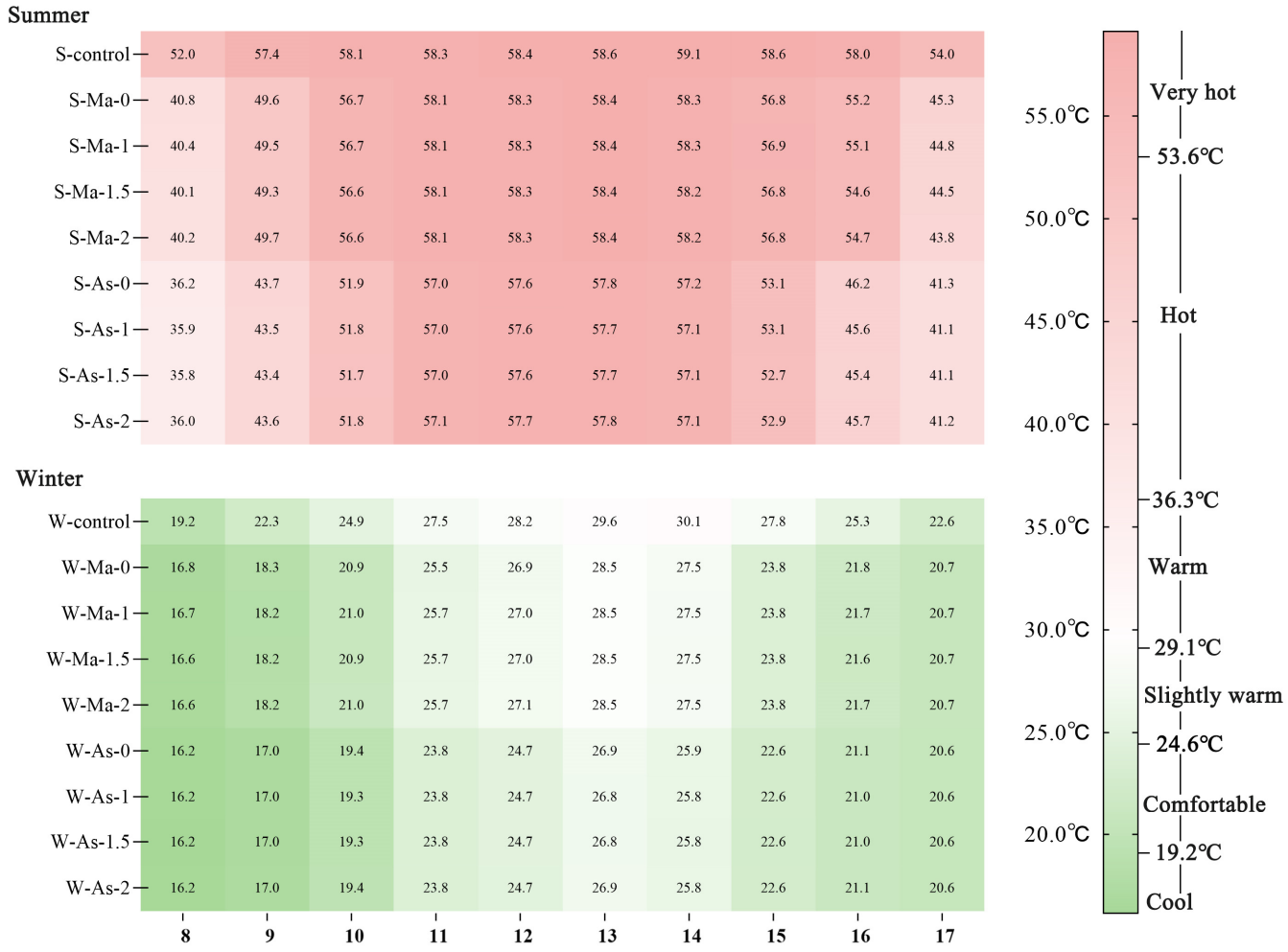

Figure 18. Distribution of PET values at shrub heights of 0, 1, 1.5, and 2 m, compared with the reference group, when As is combined with Ma.

3.5.2. Effect of Shrub Height on the Absolute $PM_{2.5}$ Concentration Difference

From the results presented in Figure 19, it can be seen that in summer, the $PM_{2.5}$ concentration in the downwind areas showed an upward trend with the shrub's height. The C value of the Qiao irrigation combination was significantly higher than that of the monoculture. Specifically, when the shrub reached 1.5 m and 2 m and combined with the As, the C values were 5.38 $\mu g/m^3$ and 5.37 $\mu g/m^3$, respectively. The results showed that higher shrubs had more obstructive effects on wind and $PM_{2.5}$, which were not conducive to the spread of $PM_{2.5}$. The C value of the combination of As and shrubs was significantly higher than that of the combination of Ma and shrubs; however, Ma was greatly affected by different shrub heights. In winter, the C values corresponding to shrubs of heights 0 m, 1 m, 1.5 m, and 2 m in both the Ma and As combination increased with shrub height. However, this growth trend was not significant and had a slight impact on the $PM_{2.5}$ concentration of the road.

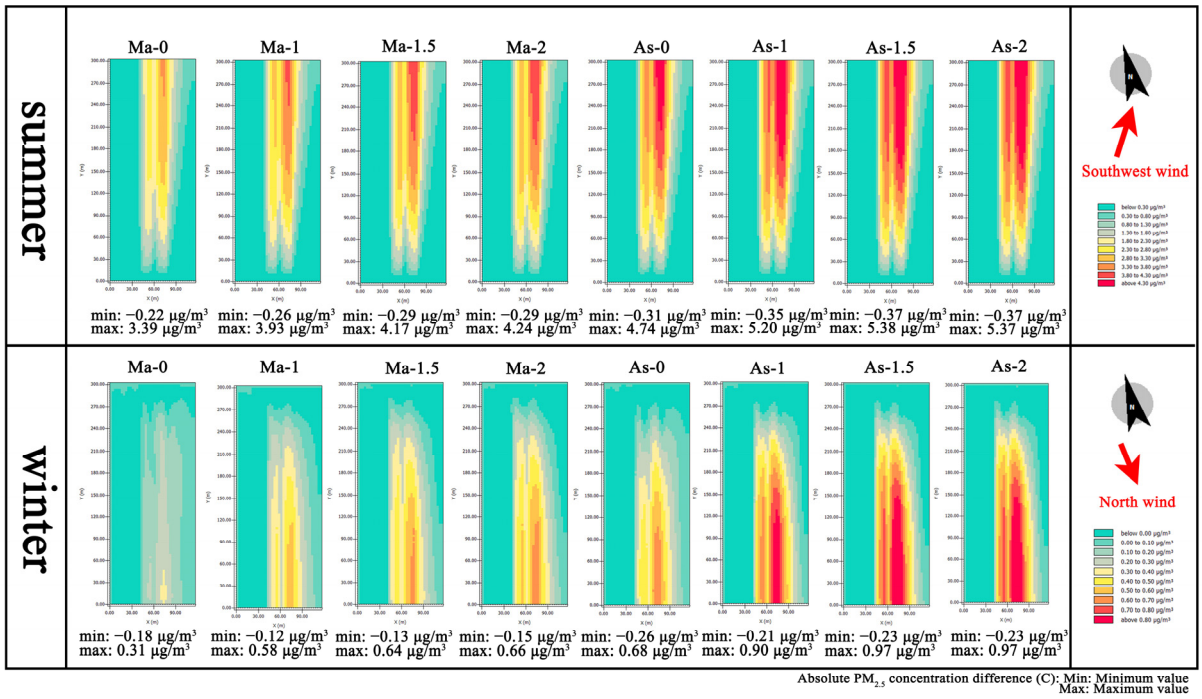

Figure 19. Absolute $PM_{2.5}$ concentration difference at shrub heights of 0, 1, 1.5, and 2 m, compared with the reference group, when As and Ma are combined.

In summary, planting shrubs under tree species that are beneficial to the spread of $PM_{2.5}$ blocks the spread of $PM_{2.5}$, thereby exacerbating air pollution to a certain extent. Increasing the height of the shrubs increased the concentration of $PM_{2.5}$, but this increase was not obvious.

4. Discussion

4.1. Impact of Plant Spacing on Thermal Comfort and $PM_{2.5}$

The results indicate that, in both summer and winter, the cooling effect of tree-planting spacing ranked as follows: 3 m > 6 m > 9 m. Specifically, the impact of varying tree planting distances on R45, which had the most greenery, showed a significant difference in PET values, with a maximum variance of 5.29 °C. This finding is consistent with that of Zhao et al. [42], who indicated that higher vegetation coverage and greenery enhance microclimate regulation. Along the north–south oriented R23 and R34 roads, the reduction in T_{mrt} ranked in the order 3 m > 6 m > 9 m. Conversely, the impact of 6 m spacing on the T_{mrt} level is most pronounced on east–southeast and west–northwest-oriented R12 and the southwest–northeast-oriented R45 roads. Huang et al. [43] highlighted that the cooling benefits of roadside trees are highly localized, with greater cooling effects observed along north–south orientations than in east–west configurations. Ian Estacio et al. [13] similarly found that urban canyons oriented east to west experienced the highest levels of heat discomfort.

Different spacing distances exhibited contrasting effects on $PM_{2.5}$ concentration and thermal comfort. These findings corroborate previous studies [13]. The results indicated that as the spacing distance increased, $PM_{2.5}$ concentration decreased in the order 3 m > 6 m > 9 m, similar to the findings by Li et al. [15], where particle concentrations increased with vegetation density. Along the R34 road, the presence of roadside trees in winter aided the reduction in $PM_{2.5}$, with slightly higher reductions observed at 3 m compared with those at 6 m and 9 m. Given the north–south orientation of R34 and the prevailing northern winds in winter, roadside trees acted as barriers against $PM_{2.5}$ diffusion from vehicular traffic, with denser trees offering more significant protection. Buccolieri et al. [44] found that under conditions where the dominant wind direction was perpendicu-

lar to the street orientation, $PM_{2.5}$ concentrations increased by 108%, while concentrations decreased by 18% when the wind direction was parallel to the street.

4.2. Effect of Tree Species on Heat Comfort and $PM_{2.5}$

Planting trees significantly reduced the PET values in pedestrian spaces; however, certain species, such as Ma, may increase the PET values during specific times. LAI, crown width, and height were the primary factors influencing vegetation cooling and ventilation [45]. The results showed that Fa and Cc effectively reduced PET values, whereas Ma and Ct showed relatively limited cooling effects. The narrow crown and high canopy base [46] of Ma inadequately shielded pedestrian areas from solar radiation [47] and hindered airflow to some extent, thereby increasing the T_{mrt} values. Notably, tree planting increased PET values in winter along R12 roadsides near buildings. This effect could be attributed to the orientation (southeast–northwest) of R12, which predominantly exposed these areas to north winds during winter. Additionally, the narrow crowns of the trees failed to provide effective shading by 2 PM, exacerbating heat absorption and prolonged release from nearby buildings [13]. Solar radiation is a primary factor influencing thermal comfort [41]. Huang et al. [43] found that trees may adversely affect wind speeds or solar exposure depending on their relationship with buildings or canopy structures. Fa effectively mitigated winter afternoon solar radiation with its broad crown and dense canopy, lowering T_{mrt} through tree-induced cooling.

The effect of tree species on $PM_{2.5}$ concentration and thermal comfort showed an opposite trend, with different tree species having different impacts on $PM_{2.5}$. The physical characteristics of trees, such as crown width, tree height, and LAI, significantly affected the concentration of $PM_{2.5}$. Among them, crown width and tree height had more significant effects. On the other hand, tree species such as Fa and Fc were unfavorable for $PM_{2.5}$ diffusion due to their physical characteristics. The small crown of Baa had the least effect on $PM_{2.5}$ concentrations in pedestrian areas. Yang et al. [48] found that higher tree heights increased concentrations. He et al. [31] also found that $PM_{2.5}$ concentrations were significantly affected by factors such as tree crown width. Excessively wide crowns and tall trees can exacerbate $PM_{2.5}$ pollution, and an increase in under-branch heights can favor $PM_{2.5}$ diffusion in the vertical direction. However, it has also been shown that the effect of trunk height on concentration changes is negligible [49]. The results of this study show that the impact of under-branch height on $PM_{2.5}$ concentration is small, which may be because this study mainly focuses on the horizontal distribution of $PM_{2.5}$ at pedestrian heights. At the same time, the tree species morphology indicator variables may not be comprehensive enough, limiting the analysis of under-branch height's effect. The study's roadway environment differed from the other studies' climatic conditions, which led to different results.

These findings underscore the significant impacts of crown width, tree height, and LAI on thermal comfort and $PM_{2.5}$ concentrations. Therefore, roadside tree species should be considered when selecting them, considering their combined effects on the thermal environment and $PM_{2.5}$.

4.3. Effect of Shrub Height on Thermal Comfort and $PM_{2.5}$

Based on the research findings, combining trees and shrubs significantly reduced PET values, with minimal impact observed from shrub height variations. Yang et al. [19] confirmed that trees markedly improved outdoor thermal comfort, whereas shrubs and ground-cover plants showed less pronounced improvements. Therefore, despite the variations in tree species, the PET values for the tree–shrub combinations were similar. In this study, planting shrubs under tree species effectively obstructed $PM_{2.5}$ dispersion, thereby potentially exacerbating air pollution to some extent. As shrub height increased, there was a slight upward trend in the downwind $PM_{2.5}$. Although shrubs obstructed $PM_{2.5}$, the increase in shrub height did not significantly increase $PM_{2.5}$.

4.4. Study Limitations

First, the simulation scenarios in this study had some limitations. In reality, wind speed and direction are constantly changing, whereas the modeled wind speed and direction are fixed, potentially contributing to the differences between simulations and measurements [21,50]. Moreover, this study employed a single pollution source in the model; however, environmental factors such as airflow and dust from vehicles can introduce additional pollutants, reflecting the diversity of real-world pollution sources [51]. Nevertheless, this study used simulations to explore the trends in $PM_{2.5}$ concentration variations influenced by different factors. Second, the research examined the effects of greenery on thermal comfort and $PM_{2.5}$ concentration across different types of roads; however, it did not account for factors such as road orientation and lane division that could affect these outcomes. In addition, this study showed that the physical characteristics of trees, such as under-branch height, had a lesser effect on $PM_{2.5}$ concentrations, but this may have been due to the lack of a comprehensive range of morphological indicators of tree species, which limited the analysis of the effect of under-branch height. Finally, the study focused solely on the dispersion effects of $PM_{2.5}$ and did not consider its deposition effects. Greenery typically has a greater impact on particle dispersion than on deposition [52]. Future research should consider varying wind speed and direction in simulations to more accurately reflect real-world conditions. Further research should consider the combined effects of environmental factors such as road orientation and traffic separation zones on thermal comfort and $PM_{2.5}$ concentrations. In addition, future studies should incorporate more morphological indicators of tree species for a comprehensive analysis.

5. Conclusions

This study comprehensively analyzed the effects of different plant spacing, tree species, and tree–shrub combinations on the thermal comfort and $PM_{2.5}$ concentration of sidewalks under hot and humid climatic conditions in summer and winter. Simulations using the validated ENVI-met model were conducted to analyze the thermal comfort and $PM_{2.5}$ concentration at pedestrian heights and provide new perspectives and data support for future related studies. Based on these analyses, the following conclusions are drawn:

1. Tree spacing had contrasting effects on the thermal environment and $PM_{2.5}$. Smaller spacings improved thermal comfort more effectively, with 3 m spacing reducing PET values by 17–20.3 °C in summer and 3.3–12.6 °C in winter. However, smaller spacings increased $PM_{2.5}$ concentrations, with maximum C values at 3 m spacing of 5.05 $\mu g/m^3$ (R45) in summer and maximum M values of 2.13 $\mu g/m^3$ (R23) in winter. This is particularly noticeable on roads with a high number of green belts.
2. Trees with wide crowns and high LAIs significantly improved thermal comfort, with reductions of up to 6.5 °C (*Ficus altissima*) in summer and 6.6 °C (*Ficus altissima*) in winter. Conversely, trees with small crowns facilitated $PM_{2.5}$. *Michelia alba* exhibited the highest C and M values at 3.39 $\mu g/m^3$ and 1.5 $\mu g/m^3$ in summer and 1.22 $\mu g/m^3$ and 0.4 $\mu g/m^3$ in winter, respectively. Planting species such as *Ficus altissima* and *Cinnamomum camphora* noticeably enhanced thermal comfort, whereas *Michelia alba* and *Chukrasia tabularis* were more effective in reducing $PM_{2.5}$.
3. Combining trees with shrubs improved thermal comfort somewhat; however, increasing shrub height resulted in higher $PM_{2.5}$. When shrub heights reached 1.5 m and 2 m in summer, C values peaked at 5.38 $\mu g/m^3$ and 5.37 $\mu g/m^3$, respectively.

Planting trees primarily for summer considerations on streets significantly impacted pedestrian comfort and $PM_{2.5}$ levels more than winter tree planting.

1. High Traffic and $PM_{2.5}$ Emission Roads: Prioritize reducing $PM_{2.5}$ pollution on busy urban expressways with dense traffic. We recommend planting *Michelia alba* and *Chukrasia tabularis* species with narrow crowns at 9 m spacing without additional shrub planting.

2. Main Urban Roads: Consider both thermal comfort and the impact of $PM_{2.5}$ on roads with high pedestrian and vehicle densities. Opt for moderate spacing like 6 m and choose species with moderate tree height, crown widths, and leaf area indices, such as *Alstonia scholaris*, *Bauhinia blakeana*, and *Dracontomelon duperreanum*.
3. Minor Urban Roads: Prioritize PET on roads with fewer vehicles and more pedestrians. Opt for closer spacing, such as 3 m or 6 m, and plant species with large crowns and high leaf area indices, such as *Ficus altissimo*, *Ficus concinna*, and *Cinnamomum camphora*. Moreover, shrubs could be added for aesthetic purposes.
4. Wind direction has a significant effect on $PM_{2.5}$ dispersion. For roads that are not parallel to the wind direction, it is recommended that diffusion-friendly tree species be planted at larger intervals, such as 9 m intervals for *Michelia alba*. If $PM_{2.5}$ pollution is more severe in summer on roads parallel to the wind direction, large spacing and diffusion-friendly tree species should be selected. If $PM_{2.5}$ pollution is more severe in winter, smaller spacing and tree species with large crowns, such as 3 m or 6 m spacing, as well as large crowns, such as *Ficus altissima*, can be selected; these will, to a certain extent, block the diffusion of $PM_{2.5}$ to the sidewalks.
5. In summary, this study investigated the effects of roadway greening design on thermal comfort and $PM_{2.5}$ concentration in hot and humid areas and made optimization recommendations. Although this study provides valuable references, future studies should consider the relevant factors more comprehensively to optimize the greening design of urban roads further to improve environmental quality.

Author Contributions: M.D.: Writing—original draft, Methodology, Formal analysis, Data curation. Y.Z.: Supervision, Methodology, Conceptualization; J.Y.: Supervision, Methodology, Conceptualization; W.W.: Data curation; X.L.: Methodology, Data curation; Z.Z.: Methodology; B.H.: Data curation. All authors have read and agreed to the published version of the manuscript.

Funding: This study was supported by the Hub Platform for Innovation in Critical Infrastructure Security and Intelligent Operation and Maintenance of Guangzhou University (grant no. PT252022006).

Institutional Review Board Statement: Not applicable.

Informed Consent Statement: Not applicable.

Data Availability Statement: Data are contained within the article and supplementary materials.

Acknowledgments: In this section, you can acknowledge any support given which is not covered by the author contribution or funding sections. This may include administrative and technical support, or donations in kind (e.g., materials used for experiments).

Conflicts of Interest: The authors declare no conflicts of interest.

Nomenclatures

LAD	leaf area density
LAIs	leaf area indices
MAE	mean absolute error
T_{mrt}	mean radiant temperature
$PM_{2.5}$	particulate matter 2.5
PET	pedestrian thermal comfort
PMV	predicted mean vote
RH	relative humidity
RMSE	root mean square error
SET	standard effective temperature
WBGT	wet bulb globe temperature
T_a	air temperature
Ws	wind speed
C	absolute $PM_{2.5}$ concentration difference
M	mean absolute $PM_{2.5}$ concentration difference
R12	one roadbed and two belts

R23	two roadways and three belts
R34	three roadways and four belts
R45	four roadways and five belts
Ma	Michelia alba
Fa	Ficus altissima
Bb	Bauhinia blakeana
Mi	Mangifera indica
As	Alstonia scholaris
Ct	Chukrasia tabularis
Dd	Dracontomelon duperreanum
Fc	Ficus concinna
Cc	Cinnamomum camphora

Appendix A

Table A1. Boundary conditions for the simulation process using the ENVI-Met model.

Boundary Conditions for the Simulation Process Using the ENVI-Met Model		
Location		Guangzhou (23°12′ N;113°20′ E)
Simulation date	Summer	September 20, September 21, September 24, September 25, 2023
	Winter	January 21, January 22, January 24, January 25, 2024
Simulation time		8:00–10:00, 11:00–14:00,15:00–17:00
Model dimensions	R12	X-Grids: 27 Y-Grids: 101 Z-Grids: 13
	R23	X-Grids: 42 Y-Grids: 102 Z-Grids: 13
	R34	X-Grids: 57 Y-Grids: 104 Z-Grids: 16
	R45	X-Grids: 39 Y-Grids: 101 Z-Grids: 15
Grid cell		dx = 3 dy = 3 dz = 3
Grid north		0
Nesting grids		5
Roughness length		0.1
Wind direction (N:0, 180:S)	R12	45 (summer) 0 (winter)
	R23	90 (summer) 0 (winter)
	R34	135 (summer) 0 (winter)
	R45	202.5 (summer) 0 (winter)
Wind speed	R12	0.8 (summer) 1.9 (winter)
	R23	0.8 (summer) 0.7 (winter)
	R34	0.8 (summer) 0.9 (winter)
	R45	0.8 (summer) 2 (winter)
Air temperature	R12	29–37.45 °C (summer) 5.4–8.3 (winter)
	R23	30.77–37.8 °C (summer) 5.5–15.5 (winter)
	R34	29.77–38.1 °C (summer) 5.1–15.9 (winter)
	R45	30.77–41.8 °C (summer) 13.8–22.6 (winter)
Relative humidity	R12	50–72% (summer) 26–33% (winter)
	R23	45–75% (summer) 20–31% (winter)
	R34	47–74% (summer) 53–64% (winter)
	R45	53–77% (summer) 44–66% (winter)
PET index calculation		Bio-met process
Results visualization		Leonardo visualization tool

Table A2. Standard deviation, variance, and coefficient of variation of measured temperature, humidity, and PM2.5 concentration during summer months.

Scene	Site	Season	Measured Parameters	Mean	Variance	Standard Deviation (SD)	Coefficient of Variation (CV)
		summer	T_a (°C)	33.291	5.333499	2.309437	6.937121
	1	summer	RH (%)	65.13	37.36233	6.112474	9.385035
		summer	$PM_{2.5}$ ($\mu g/m^3$)	20.10667	24.83179	4.983151	24.78357
		summer	T_a (°C)	33.965	3.716917	1.927931	5.676227
R12	2	summer	RH (%)	60.44	73.08933	8.54923	14.14499
		summer	$PM_{2.5}$ ($\mu g/m^3$)	20.10667	24.83179	4.983151	24.78357
		summer	T_a (°C)	36.146	8.217538	2.866625	7.930683
	3	summer	RH (%)	59.09	54.90767	7.409971	12.54014
		summer	$PM_{2.5}$ ($\mu g/m^3$)	20.55333	22.44425	4.737537	23.04997
		summer	T_a (°C)	35.305	4.779406	2.186185	6.192282
	1	summer	RH (%)	58.04	77.06267	8.778534	15.12497
		summer	$PM_{2.5}$ ($\mu g/m^3$)	26.24	52.61896	7.253893	27.64441
		summer	T_a (°C)	35.074	7.587471	2.754536	7.8535
R23	2	summer	RH (%)	63.21	59.32544	7.702301	12.18526
		summer	$PM_{2.5}$ ($\mu g/m^3$)	26.51	81.63828	9.035391	34.08295
		summer	T_a (°C)	37.36	2.100156	1.449191	3.878992
	3	summer	RH (%)	57.28	42.60622	6.527344	11.3955
		summer	$PM_{2.5}$ ($\mu g/m^3$)	24.91333	42.28967	6.503051	26.10269
		summer	T_a (°C)	34.469	8.515254	2.918091	8.465841
	1	summer	RH (%)	63.14	57.20489	7.563391	11.97876
		summer	$PM_{2.5}$ ($\mu g/m^3$)	28.1814	70.57995	8.401188	29.81111
		summer	T_a (°C)	35.844	7.686716	2.772493	7.734886
R34	2	summer	RH (%)	58.79	29.95656	5.473258	9.309846
		summer	$PM_{2.5}$ ($\mu g/m^3$)	27.56552	84.59892	9.197767	33.36693
		summer	T_a (°C)	37.125	3.710783	1.926339	5.188793
	3	summer	RH (%)	63.83	22.05789	4.696583	7.357955
		summer	$PM_{2.5}$ ($\mu g/m^3$)	27.52	79.55388	8.919298	32.41024
		summer	T_a (°C)	35.233	5.124401	2.263714	6.424982
	1	summer	RH (%)	61.45	20.10722	4.484108	7.297165
		summer	$PM_{2.5}$ ($\mu g/m^3$)	25.87	42.16554	6.4935	25.1005
		summer	T_a (°C)	33.257	6.020823	2.453737	7.378106
R45	2	summer	RH (%)	67.34	7.962667	2.82182	4.190407
		summer	$PM_{2.5}$ ($\mu g/m^3$)	27.29444	22.13242	4.704511	17.23615
		summer	T_a (°C)	36.92	5.445156	2.333486	6.320384
	3	summer	RH (%)	62.26	17.31822	4.161517	6.684094
		summer	$PM_{2.5}$ ($\mu g/m^3$)	27.26816	34.16276	5.844892	21.43486

Table A3. Standard deviation, variance, and coefficient of variation of measured temperature, humidity, and PM2.5 concentrations in winter.

Scene	Site	Season	Measured Parameters	Mean	Variance	Standard Deviation (SD)	Coefficient of Variation (CV)
		winter	T_a (°C)	6.7233	1.820863	1.349394	20.07041
	1	winter	RH (%)	45.1866	5.740936	2.396025	5.302512
		winter	$PM_{2.5}$ ($\mu g/m^3$)	35.84	1.711556	1.308264	3.650291
		winter	T_a (°C)	7.437	1.683201	1.297382	17.44497
R12	2	winter	RH (%)	61.16	1.698222	1.303159	2.130737
		winter	$PM_{2.5}$ ($\mu g/m^3$)	36.03	0.793444	0.890755	2.472259
		winter	T_a (°C)	8.859	3.304299	1.817773	20.51894
	3	winter	RH (%)	42.68	11.21067	3.348233	7.84497
		winter	$PM_{2.5}$ ($\mu g/m^3$)	36.1	1.073333	1.036018	2.869856
		winter	T_a (°C)	11.425	10.05647	3.171194	27.75662
	1	winter	RH (%)	59.06	2.147111	1.465302	2.48104
		winter	$PM_{2.5}$ ($\mu g/m^3$)	38.14	2.876	1.695877	4.446453
		winter	T_a (°C)	11.482	7.191742	2.681742	23.35606
R23	2	winter	RH (%)	41.7134	19.38863	4.403252	10.55597
		winter	$PM_{2.5}$ ($\mu g/m^3$)	37.06	5.751556	2.39824	6.471236
		winter	T_a (°C)	12.713	17.55949	4.190405	32.96157
	3	winter	RH (%)	40.7	33.11333	5.754419	14.13862
		winter	$PM_{2.5}$ ($\mu g/m^3$)	38.62	3.892889	1.973041	5.108857

Table A3. *Cont.*

Scene	Site	Season	Measured Parameters	Mean	Variance	Standard Deviation (SD)	Coefficient of Variation (CV)
R34	1	winter	T_a (°C)	10.6074	1.268156	1.126125	10.61641
		winter	RH (%)	73.761	7.155227	2.674926	3.626477
		winter	$PM_{2.5}$ ($\mu g/m^3$)	10.98	140.2329	11.842	107.8506
	2	winter	T_a (°C)	10.815	1.726806	1.31408	12.15053
		winter	RH (%)	68.14	1.009333	1.004656	1.4744
		winter	$PM_{2.5}$ ($\mu g/m^3$)	11.79778	141.7642	11.90648	100.9214
	3	winter	T_a (°C)	10.986	1.715738	1.309862	11.92301
		winter	RH (%)	64.85	13.91389	3.730133	5.751939
		winter	$PM_{2.5}$ ($\mu g/m^3$)	12.41	144.9921	12.04127	97.02874
R45	1	winter	T_a (°C)	19.388	11.95355	3.457391	17.83263
		winter	RH (%)	66.03	12.15344	3.486179	5.27969
		winter	$PM_{2.5}$ ($\mu g/m^3$)	29.5	6.302222	2.510423	8.509908
	2	winter	T_a (°C)	17.3311	8.960809	2.993461	17.27219
		winter	RH (%)	60.1699	55.81766	7.471121	12.41671
		winter	$PM_{2.5}$ ($\mu g/m^3$)	30.54	5.611556	2.368872	7.756622
	3	winter	T_a (°C)	20.682	20.526	4.530562	21.90582
		winter	RH (%)	46.84	65.67378	8.103936	17.30131
		winter	$PM_{2.5}$ ($\mu g/m^3$)	30.39	4.912111	2.216328	7.292953

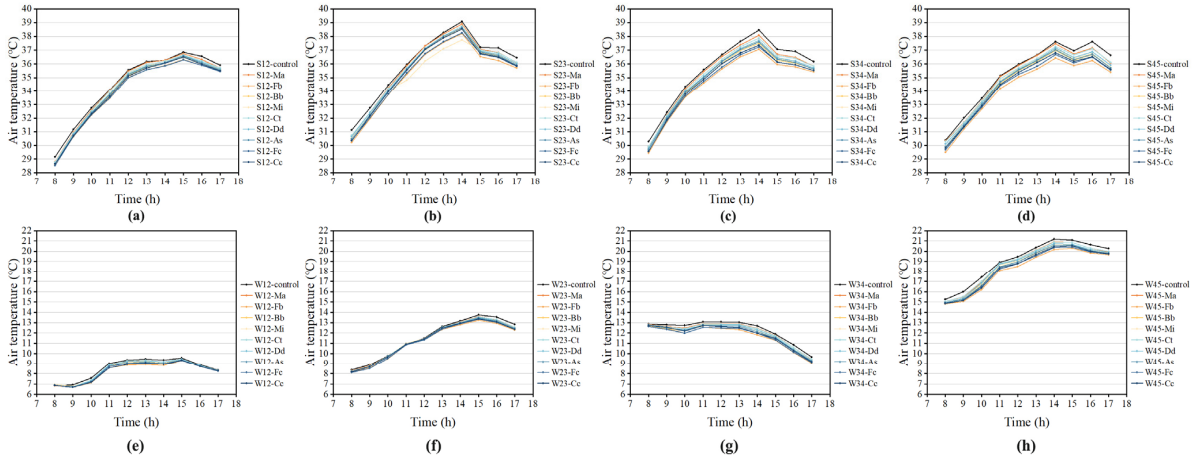

Figure A1. Effects of the T_a species on the T_a of R12, R23, R34, and R45 during summer (**a**–**d**) and winter (**e**–**h**).

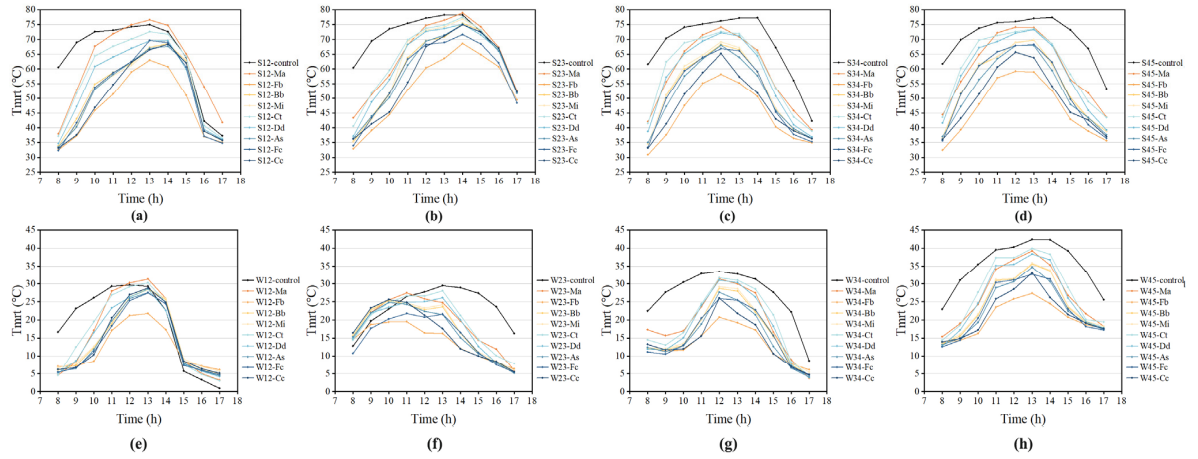

Figure A2. Effects of tree species on the T_{mrt} of R12, R23, R34, and R45 during summer (**a**–**d**) and winter (**e**–**h**).

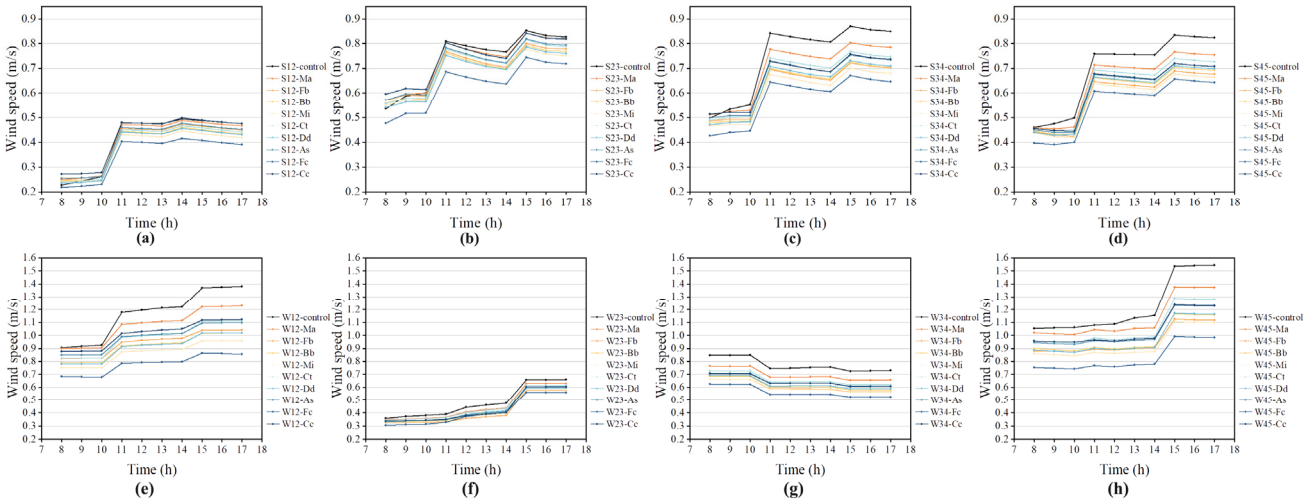

Figure A3. Effects of tree species on the Ws of R12, R23, R34, and R45 during summer (**a**–**d**) and winter (**e**–**h**).

References

1. Banerjee, S.; Ching, N.Y.G.; Yik, S.K.; Dzyuban, Y.; Crank, P.J.; Yi, R.P.X.; Chow, W.T.L. Analysing impacts of urban morphological variables and density on outdoor microclimate for tropical cities: A review and a framework proposal for future research directions. *Build. Environ.* **2022**, *225*, 109646. [CrossRef]
2. Xu, T.; Song, Y.; Liu, M.; Cai, X.; Zhang, H.; Guo, J.; Zhu, T. Temperature inversions in severe polluted days derived from radiosonde data in North China from 2011 to 2016. *Sci. Total Environ.* **2019**, *647*, 1011–1020. [CrossRef] [PubMed]
3. Guo, Y.M.; Gasparrini, A.; Li, S.S.; Sera, F.; Vicedo-Cabrera, A.M.; Coelho, M.; Saldiva, P.H.N.; Lavigne, E.; Tawatsupa, B.; Punnasiri, K.; et al. Quantifying excess deaths related to heatwaves under climate change scenarios: A multicountry time series modelling study. *PLoS Med.* **2018**, *15*, e1002629. [CrossRef] [PubMed]
4. Dab, W.; Ségala, C.; Dor, F.; Festy, B.; Lameloise, P.; Le Moullec, Y.; Le Tertre, A.; Médina, S.; Quénel, P.; Wallaert, B.; et al. Air pollution and health: Correlation or casuality?: The case of the relationship between particle exposure and deaths from heart and lung disease. *J. Air Waste Manag. Assoc.* **2001**, *51*, 203–219. [CrossRef] [PubMed]
5. Li, C.G.; Lin, T.; Zhang, Z.F.; Xu, D.; Huang, L.; Bai, W.P. Can transportation infrastructure reduce haze pollution in China? *Environ. Sci. Pollut. Res.* **2022**, *29*, 15564–15581. [CrossRef]
6. Karagulian, F.; Belis, C.A.; Dora, C.F.C.; Prüss-Ustün, A.M.; Bonjour, S.; Adair-Rohani, H.; Amann, M. Contributions to cities' ambient particulate matter (PM): A systematic review of local source contributions at global level. *Atmos. Environ.* **2015**, *120*, 475–483. [CrossRef]
7. Hill, W.; Lim, E.L.; Weeden, C.E.; Lee, C.; Augustine, M.; Chen, K.; Kuan, F.C.; Marongiu, F.; Evans, E.J.; Moore, D.A.; et al. Lung adenocarcinoma promotion by air pollutants. *Nature* **2023**, *616*, 159–167. [CrossRef]
8. Zheng, G.Z.; Zhu, N.; Tian, Z.; Chen, Y.; Sun, B.H. Application of a trapezoidal fuzzy AHP method for work safety evaluation and early warning rating of hot and humid environments. *Saf. Sci.* **2012**, *50*, 228–239. [CrossRef]
9. Sæbo, A.; Popek, R.; Nawrot, B.; Hanslin, H.M.; Gawronska, H.; Gawronski, S.W. Plant species differences in particulate matter accumulation on leaf surfaces. *Sci. Total Environ.* **2012**, *427*, 347–354. [CrossRef]
10. Salim, M.H.; Schlünzen, K.H.; Grawe, D. Including trees in the numerical simulations of the wind flow in urban areas: Should we care? *J. Wind Eng. Ind. Aerodyn.* **2015**, *144*, 84–95. [CrossRef]
11. Vos, P.E.J.; Maiheu, B.; Vankerkom, J.; Janssen, S. Improving local air quality in cities: To tree or not to tree? *Environ. Pollut.* **2013**, *183*, 113–122. [CrossRef] [PubMed]
12. Yang, J.; Zhao, Y.; Guo, T.; Luo, X.; Ji, K.; Zhou, M.; Wan, F. The impact of tree species and planting location on outdoor thermal comfort of a semi-outdoor space. *Int. J. Biometeorol.* **2023**, *67*, 1689–1701. [CrossRef] [PubMed]
13. Estacio, I.; Hadfi, R.; Blanco, A.; Ito, T.; Babaan, J. Optimization of tree positioning to maximize walking in urban outdoor spaces: A modeling and simulation framework. *Sustain. Cities Soc.* **2022**, *86*, 104105. [CrossRef]
14. Park, C.Y.; Lee, D.K.; Krayenhoff, E.S.; Heo, H.K.; Hyun, J.H.; Oh, K.; Park, T.Y. Variations in pedestrian mean radiant temperature based on the spacing and size of street trees. *Sustain. Cities Soc.* **2019**, *48*, 101521. [CrossRef]
15. Li, Z.T.; Zhang, H.; Juan, Y.H.; Lee, Y.T.; Wen, C.Y.; Yang, A.S. Effects of urban tree planting on thermal comfort and air quality in the street canyon in a subtropical climate. *Sustain. Cities Soc.* **2023**, *91*, 104334. [CrossRef]
16. Wania, A.; Bruse, M.; Blond, N.; Weber, C. Analysing the influence of different street vegetation on traffic-induced particle dispersion using microscale simulations. *J. Environ. Manag.* **2012**, *94*, 91–101. [CrossRef]
17. Yao, Y.B.; Chang, J.; Yang, H.Y.; Jie, B. Current status and development trend of landscape visual environment quality evaluation research. *J. West Anhui Univ.* **2021**, *37*, 110–119.

18. Salmond, J.A.; Williams, D.E.; Laing, G.; Kingham, S.; Dirks, K.; Longley, I.; Henshaw, G.S. The influence of vegetation on the horizontal and vertical distribution of pollutants in a street canyon. *Sci. Total Environ.* **2013**, *443*, 287–298. [CrossRef]
19. Yang, Y.J.; Zhou, D.; Wang, Y.P.; Ma, D.X.; Chen, W.; Xu, D.; Zhu, Z.Z. Economical and outdoor thermal comfort analysis of greening in multistory residential areas in Xi'an. *Sustain. Cities Soc.* **2019**, *51*, 101730. [CrossRef]
20. Li, J.Y.; Zheng, B.H.; Ouyang, X.; Chen, X.; Bedra, K.B. Does shrub benefit the thermal comfort at pedestrian height in Singapore? *Sustain. Cities Soc.* **2021**, *75*, 103333. [CrossRef]
21. Wu, J.S.; Luo, K.Y.; Wang, Y.; Wang, Z.Y. Urban road greenbelt configuration: The perspective of $PM_{2.5}$ removal and air quality regulation. *Environ. Int.* **2021**, *157*, 106786. [CrossRef] [PubMed]
22. Chen, X.; Wu, J.; Yang, W.B.; Wang, Z.Y.; Chen, S.T.; Hu, X.S.; Lu, K.F.; Fan, Z.M.; Lin, M.; Chen, P. Measuring and modeling the effects of green barriers on the spatial distribution of fine particulate matter at roadside. *Urban Clim.* **2023**, *52*, 101727. [CrossRef]
23. Ali-Toudert, F.; Mayer, H. Effects of asymmetry, galleries, overhanging facades and vegetation on thermal comfort in urban street canyons. *Sol. Energy* **2007**, *81*, 742–754. [CrossRef]
24. Lin, P.Y.; Song, D.X.; Qin, H. Impact of parking and greening design strategies on summertime outdoor thermal condition in old mid-rise residential estates. *Urban For. Urban Green.* **2021**, *63*, 127200. [CrossRef]
25. Xiong, Y.Z.; Huang, S.P.; Chen, F.; Ye, H.; Wang, C.P.; Zhu, C.B. The Impacts of Rapid Urbanization on the Thermal Environment: A Remote Sensing Study of Guangzhou, South China. *Remote Sens.* **2012**, *4*, 2033–2056. [CrossRef]
26. Zhou, K.; Ye, Y.H.; Liu, Q.; Liu, A.J.; Peng, S.L. Evaluation of ambient air quality in Guangzhou, China. *J. Environ. Sci.* **2007**, *19*, 432–437. [CrossRef]
27. Li, K.M.; Zhang, Y.F.; Zhao, L.H. Outdoor thermal comfort and activities in the urban residential community in a humid subtropical area of China. *Energy Build.* **2016**, *133*, 498–511. [CrossRef]
28. Yang, X.S.; Zhao, L.H.; Bruse, M.; Meng, Q.L. Evaluation of a microclimate model for predicting the thermal behavior of different ground surfaces. *Build. Environ.* **2013**, *60*, 93–104. [CrossRef]
29. Wang, B. Study on optimization strategy of road greening in the central urban area of Zengcheng District, Guangzhou City, China. Master's Thesis, South China University of Technology, Guangzhou, China, 2020.
30. Järvi, L.; Kurppa, M.; Kuuluvainen, H.; Rönkkö, T.; Karttunen, S.; Balling, A.; Timonen, H.; Niemi, J.; Pirjola, L. Determinants of spatial variability of air pollutant concentrations in a street canyon network measured using a mobile laboratory and a drone. *Sci. Total Environ.* **2023**, *856*, 158974. [CrossRef]
31. He, H.Y.; Zhu, Y.S.; Liu, L.; Du, J.; Liu, L.R.; Liu, J. Effects of roadside trees three-dimensional morphology characteristics on traffic-related PM2.5 distribution in hot-humid urban blocks. *Urban Clim.* **2023**, *49*, 101448. [CrossRef]
32. Dai, S.; Bi, X.; Chan, L.Y.; He, J.; Wang, B.; Wang, X.; Peng, P.; Sheng, G.; Fu, J. Chemical and stable carbon isotopic composition of $PM_{2.5}$ from on-road vehicle emissions in the PRD region and implications for vehicle emission control policy. *Atmos. Chem. Phys.* **2015**, *15*, 3097–3108. [CrossRef]
33. Liu, J.Y.; Zheng, B.H. A Simulation Study on the Influence of Street Tree Configuration on Fine Particulate Matter ($PM_{2.5}$) Concentration in Street Canyons. *Forests* **2023**, *14*, 1550. [CrossRef]
34. Liu, Z.; Tan, G.; Zhao, L. Simplification Method for Building Tree Models in ENVI-met: A Case Study of Ficus microcarpa. *Guangdong Landsc. Arch.* **2018**, *46*, 83–87.
35. Lalic, B.; Mihailovic, D.T. An empirical relation describing leaf-area density inside the forest for environmental modeling. *J. Appl. Meteorol.* **2004**, *43*, 641–645. [CrossRef]
36. Fang, Z.S.; Feng, X.W.; Liu, J.L.; Lin, Z.; Mak, C.M.; Niu, J.L.; Tse, K.T.; Xu, X.N. Investigation into the differences among several outdoor thermal comfort indices against field survey in subtropics. *Sustain. Cities Soc.* **2019**, *44*, 676–690. [CrossRef]
37. Zhang, L.L.L.; Wei, D.; Hou, Y.Y.; Du, J.F.; Liu, Z.; Zhang, G.M.; Shi, L. Outdoor Thermal Comfort of Urban Park—A Case Study. *Sustainability* **2020**, *12*, 1961. [CrossRef]
38. Lin, T.-P.; Matzarakis, A. Tourism climate and thermal comfort in Sun Moon Lake, Taiwan. *Int. J. Biometeorol.* **2008**, *52*, 281–290. [CrossRef]
39. Fang, Z.; Feng, X.; Xu, X.; Zhou, X.; Lin, Z.; Ji, Y. Investigation into outdoor thermal comfort conditions by different seasonal field surveys in China, Guangzhou. *Int. J. Biometeorol.* **2019**, *63*, 1357–1368. [CrossRef]
40. Polednik, B.; Piotrowicz, A. Pedestrian exposure to traffic-related particles along a city road in Lublin, Poland. *Atmos. Pollut. Res.* **2020**, *11*, 686–692. [CrossRef]
41. Jung, S.J.; Yoon, S. Effects of Creating Street Greenery in Urban Pedestrian Roads on Microclimates and Particulate Matter Concentrations. *Sustainability* **2022**, *14*, 7887. [CrossRef]
42. Zhao, D.; Lei, Q.H.; Shi, Y.J.; Wang, M.D.; Chen, S.B.; Shah, K.; Ji, W.L. Role of Species and Planting Configuration on Transpiration and Microclimate for Urban Trees. *Forests* **2020**, *11*, 825. [CrossRef]
43. Huang, J.M.; Chen, L.C. Synergistic Effects of Roadside Trees and Spatial Geometry on Thermal Environment in Urban Streets: A Case Study in Tropical, Medium-Sized City, Taiwan. *Buildings* **2023**, *13*, 2092. [CrossRef]
44. Buccolieri, R.; Jeanjean, A.P.R.; Gatto, E.; Leigh, R.J. The impact of trees on street ventilation, NO_x and $PM_{2.5}$ concentrations across heights in Marylebone Rd street canyon, central London. *Sustain. Cities Soc.* **2018**, *41*, 227–241. [CrossRef]
45. Zhang, L.; Zhan, Q.M.; Lan, Y.L. Effects of the tree distribution and species on outdoor environment conditions in a hot summer and cold winter zone: A case study in Wuhan residential quarters. *Build. Environ.* **2018**, *130*, 27–39. [CrossRef]

46. Zhang, J.; Gou, Z.H. Tree crowns and their associated summertime microclimatic adjustment and thermal comfort improvement in urban parks in a subtropical city of China. *Urban For. Urban Green.* **2021**, *59*, 126912. [CrossRef]
47. Pace, R.; De Fino, F.; Rahman, M.A.; Pauleit, S.; Nowak, D.J.; Grote, R. A single tree model to consistently simulate cooling, shading, and pollution uptake of urban trees. *Int. J. Biometeorol.* **2021**, *65*, 277–289. [CrossRef]
48. Yang, H.; Chen, T.; Lin, Y.; Buccolieri, R.; Mattsson, M.; Zhang, M.; Hang, J.; Wang, Q. Integrated impacts of tree planting and street aspect ratios on CO dispersion and personal exposure in full-scale street canyons. *Build. Environ.* **2020**, *169*, 106529. [CrossRef]
49. Morakinyo, T.E.; Lam, Y.F. Study of traffic-related pollutant removal from street canyon with trees: Dispersion and deposition perspective. *Environ. Sci. Pollut. Res.* **2016**, *23*, 21652–21668. [CrossRef]
50. Abhijith, K.V.; Kumar, P.; Gallagher, J.; McNabola, A.; Baldauf, R.; Pilla, F.; Broderick, B.; Di Sabatino, S.; Pulvirenti, B. Air pollution abatement performances of green infrastructure in open road and built-up street canyon environments—A review. *Atmos. Environ.* **2017**, *162*, 71–86. [CrossRef]
51. Deng, S.X.; Ma, J.; Zhang, L.L.; Jia, Z.K.; Ma, L.Y. Microclimate simulation and model optimization of the effect of roadway green space on atmospheric particulate matter. *Environ. Pollut.* **2019**, *246*, 932–944. [CrossRef]
52. Baldauf, R. Roadside vegetation design characteristics that can improve local, near-road air quality. *Transp. Res. Part D-Transp. Environ.* **2017**, *52*, 354–361. [CrossRef] [PubMed]